# PHYSICAL BILLIARDS AND OPEN DYNAMICAL SYSTEMS

A Dissertation
Presented to
The Academic Faculty

By

Hassan Attarchi

In Partial Fulfillment
of the Requirements for the Degree
Doctor of Philosophy in the
School of Mathematics

Georgia Institute of Technology

August 2021

**PHYSICAL BILLIARDS AND OPEN DYNAMICAL SYSTEMS**

Thesis committee:


Dr. Leonid A. Bunimovich
School of Mathematics
*Georgia Institute of Technology*

Dr. Yingjie Liu
School of Mathematics
*Georgia Institute of Technology*

Dr. Federico Bonetto
School of Mathematics
*Georgia Institute of Technology*

Dr. Yao Yao
School of Mathematics
*Georgia Institute of Technology*

Dr. Predrag Cvitanović
Department of Physics
*Georgia Institute of Technology*



Date approved: July, 2021

To my parents

## ACKNOWLEDGMENTS

Foremost, I would like to express my sincere gratitude to my advisor Prof. Leonid A. Bunimovich for the continuous support of my Ph.D. study and research, for his patience, motivation, enthusiasm, and immense knowledge. His guidance helped me in all the time of research and writing of this thesis. I could not have imagined having a better advisor and mentor for my Ph.D. study.

Besides my advisor, I would like to thank the rest of my thesis committee: Prof. Federico Bonetto, Prof. Predrag Cvitanovic, Prof. Yingjie Liu, and Prof. Yao Yao for their encouragement and insightful comments.

Special thanks are due to the friends and colleagues who made this work possible: Surena Hozoori, Adrian Perez Bustamante, Hossein Talebinezhad, Sergio Mayorga, Raha Rastegar, and Haiyu Zou. They were invaluable both as friends and as sounding boards for some of my more outlandish ideas.

## TABLE OF CONTENTS

## LIST OF TABLES

## LIST OF FIGURES

## SUMMARY

This thesis consists of four works in dynamical systems with a focus on billiards. In the first part, we consider open dynamical systems, where there exists at least a "hole" of positive measure in the phase space which some portion of points in phase space escapes through that hole at each iterate of the dynamical system map. Here, we study the escape rate (a quantity that presents at what rate points in phase space escape through the hole) and various estimations of the escape rate of an open dynamical system. We uncover a reason why the escape rate is faster than expected, which is the convexity of the function defining escape rate. Moreover, exact computations of escape rate and its estimations are present for the skewed tent map and Arnold's cat map.

In the second part of the thesis, we study physical billiards where the moving particle has a finite nonzero size. In contrast to mathematical billiards where a trajectory is excluded when it hits a corner point of the boundary, in physical billiards reflection of the physical particle (a ball) off a visible corner point is well-defined. Initially, we study properties of such reflections in a physical billiards. Our results confirm that the reflection considered in the literature about physical billiards are indeed no-slip friction-free (elastic) collisions.

In the third part of the thesis, we study physical Ehrenfests' wind-tree models, where we show that physical wind-tree models are dynamically richer than the well-known Lorentz gas model. More precisely, when we replace the point particle by a physical one (a ball), the wind-tree models show a new superdiffusive regimes that never been observed in any other model such as Lorentz gas.

Finally, we prove that typical physical polygonal billiard is hyperbolic at least on a subset of positive measure and therefore has a positive Kolmogorov-Sinai entropy for any positive radius of the moving particle.

# CHAPTER 1
# INTRODUCTION

A billiard in a region $Q$ of $\mathbb{R}^n$ is the dynamical system generated by the uniform linear motion of a point particle inside $Q$ with unit speed and with elastic reflections at $\partial Q$ according to the rule that the angle of reflection equals the angle of incidence. The mathematical theory of these systems was pioneered by Birkhoff and later Sinai and many others [1, 2, 3].

The focus of this thesis is on planar billiards, where $Q$ is a domain in $\mathbb{R}^2$, and it has piecewise $C^2$ boundary components. We consider inwards unit normal vectors to the boundary components of $Q$. With respect to these normal vectors, we can define signed curvature of the boundary. Then, there are three types of the boundary points: focusing, dispersing, and neutral (flat) where the curvature is negative, positive, and zero, respectively. The boundary of a billiard table may have some singularities where the boundary has no normal vector at those points (boundary is $C^0$ at singularities). It is easy to see that the set of orbits which hit singular points of the boundary of a billiard table has measure zero with respect to the natural invariant measure on the phase space.

Note that, the boundary of a billiard table at the intersection point of two boundary components can be $C^1$ where the inwards normal vector exists; however, the curvature is not continuous at this point. Therefore, the trajectories that hit such points are well-defined, and one can study its evolution in the system.

Mathematical billiards serve as relevant models of various phenomena in mechanics, geometric optics and acoustics, statistical physics, and quantum physics [4, 5, 6, 7, 8]. Such billiards also constitute one of the most popular and arguably the most visual class of dynamical systems in the mathematical studies. Billiards exhibit a wide spectrum of different dynamical behaviors from integrable to completely chaotic systems which well repre-

sents the variety of the behaviors of conservative systems. More precisely, the dynamics of billiards is completely defined by the shape of its boundary. For example, billiards in elliptical tables are integrable, and their phase space is foliated by invariant curves where orbits corresponding to the leaves of the foliation are periodic or quasi-periodic. On the contrary, Sinai's billiards, which are billiards with boundary components of positive curvature, are hyperbolic. There are many examples of billiard tables without any boundary components of positive curvature that they can produce hyperbolic billiards as well, the most famous example of such tables is the stadium. A generic billiard table is neither fully integrable nor fully hyperbolic. Their phase space decomposes in two invariant subsets of positive measure: stable islands and chaotic seas.

For a long time, only mathematical billiards were considered, where a point (mathematical) particle moves. There are no and there will be no such particles in reality. Nevertheless, studies of just mathematical billiards were considered to be sufficient. The reasons for that were twofold. First, a system with real (finite size) particles could be sometimes reduced to a mathematical (point particle) billiard in some peculiar billiard table. Such situation takes place for instance for celebrated Boltzmann gas of hard spheres [9]. Moreover, all basic examples of billiards with regular dynamics (e.g. billiards in circles and rectangles) have absolutely the same dynamics if one considers a hard disc moving within the same billiard table. The same happens to the most popular chaotic (hyperbolic) billiards like Sinai billiards and squashes (stadium is a special case of a squash) [3, 10].

In this thesis, we mainly consider physical billiards where the moving particle is a hard ball. In [10], it was shown that in the transition from a mathematical to a physical billiard in the same billiard table any type of transition from chaotic to regular dynamics and vice versa may occur. Moreover, such transition from the point to a finite size particle can completely change the dynamics of some classical and well-studied models like e.g. the Ehrenfests' Wind-Tree model [11]. In quantum systems, a "particle" naturally has a finite size due to the uncertainty principle which leads to some new findings in the quantum chaos

theory [12, 13].

Another focus of this thesis is on open dynamical systems. Mathematical studies of open dynamical systems started in 1979 [14], where a natural question was raised about what is going to happen if in a billiard table will appear a hole through which a billiard ball can fall.

Two exact mathematical questions were formulated in [14]. First of all, one should consider a mathematical billiard where a point (mathematical) particle moves. Billiards are Hamiltonian systems and therefore a natural (physical) measure (phase space volume) is preserved under dynamics. But, what if there is a "hole" of positive measure, otherwise probability to reach a hole is zero? Would be there then a natural invariant measure for this open system? Such measures are called conditionally invariant measures. They are characterized by the property that at each iterate of the map the same portion of the remaining in the phase space points escapes through the hole. The real interest, though, is only absolutely continuous conditionally invariant measures (a.c.c.i.m.) [15]. Another question was about the existence of a natural quantity that characterizes the dynamics of open systems. Such characteristic is the escape rate of orbits through a hole [15].

Of course, physicists studied open systems long before mathematicians [16]. It was noticed in real and numerical experiments that escape from chaotic systems is an exponential function of time. Therefore, the factor in front of time in this exponent was naturally called the escape rate. And mathematically the escape rate is defined in the same way.

The organisation of the thesis is as follows. In Chapter 2, we consider chaotic (hyperbolic) dynamical systems which have a generating Markov partition. Then, open dynamical systems are built by making one element of a Markov partition a "hole" through which orbits escape. We compare various estimates of the escape rate which correspond to a physical picture of leaking in the entire phase space. Moreover, we uncover a reason why the escape rate is faster than expected, which is the convexity of the function defining escape rate. Exact computations are present for the skewed tent map and Arnold's cat map.

In Chapter 3, we consider the collision of a hard ball with a visible singular point and demonstrate that the motion of the smooth ball after collision with a visible singular point is indeed the one that was used in the studies of physical billiards. So such collision is equivalent to the elastic reflection of hard ball's center off a sphere with the center at the singular point and the same radius as the radius of the moving particle. However, a ball could be rough, not smooth. In difference with a smooth ball, a rough ball also acquires rotation after reflection off a point of the boundary which leads to more complicated dynamics.

In Chapter 4, we consider a physical Ehrenfests' Wind-Tree model where a moving particle is a hard ball rather than (mathematical) point particle. We demonstrate that a physical periodic Wind-Tree model is dynamically richer than a physical or mathematical periodic Lorentz gas. Namely, the physical Wind-Tree model may have diffusive behavior as the Lorentz gas does, but it has more superdiffusive regimes than the Lorentz gas. The new superdiffusive regime where the diffusion coefficient $D(t) \sim (\ln t)^2$ of dynamics seems to be never observed before in any model.

In Chapter 5, we will study physical billiards in generic polygonal billiards. It is well-known that billiards in polygons cannot be chaotic (hyperbolic). Particularly Kolmogorov-Sinai entropy of any polygonal billiard is zero. We consider physical polygonal billiards where a moving particle is a hard disc rather than a point (mathematical) particle and show that typical physical polygonal billiard is hyperbolic at least on a subset of positive measure and therefore has a positive Kolmogorov-Sinai entropy for any positive radius of the moving particle (provided that the particle is not so big that it cannot move within a polygon). This happens because a typical physical polygonal billiard is equivalent to a mathematical (point particle) semi-dispersing billiard.

The results of the thesis were published in the papers [17, 18, 11, 19], respectively, as they appear in the content of this thesis.

## CHAPTER 2

## WHY ESCAPE IS FASTER THAN EXPECTED

For a long time, the mathematical theory of open systems was dealing essentially with two tasks, which are proving the existence of conditionally invariant measures and the existence of escape rates. A comprehensive description of these efforts is presented in [15]. The situation changed when a new natural question was put forth in [20], which asks how the process of escape depends on the position of a hole in the phase space? Thanks to emerging research from this question, several fundamental and seemingly obvious previously existing beliefs were rigorously proved to be wrong.

First of all, even in the most uniformly hyperbolic (homogeneously expanding distances in the phase space) dynamical systems, the escape rate demonstrates strong oscillations when holes are placed at the different parts of the phase space. A natural example is the doubling map of the unit interval $f(x) = 2x \ (mod\ 1)$ where at each point, besides $x = 1/2$, dynamics expands distances twice. The most striking result in this direction though is that in a typical ergodic system, observe that just ergodic rather than strongly chaotic systems are considered here, there is a continuum of huge "holes" through which the escape rate is arbitrarily small. The sizes (probabilities, measures) of these holes are arbitrarily close to the size of the entire phase space [20, 21]. Therefore, the notion of the escape rate, although seemingly being so simple and clear, should be taken with great care in theoretical and experimental studies.

Another indication of this was an unexpected observation made in [22] for a doubling map. In [22], it was demonstrated that the average over elements of a Markov partition of escape rates is larger than expected. It is a surprising result in view of [20] where it was shown that for the doubling map the escape rate becomes smaller near periodic points. Namely, the escape rate behaves like a constant $C$ times the size of "hole" when

a hole shrinks to a non-periodic (periodic) point, where $C = 1$ ($C < 1$). This result was generalized to large classes of maps in [23, 24].

Having in mind these results, it was natural to assume that a commonly used in physics studies (so-called "naive") estimate of the escape rate [16] should be greater than the average of escape rates taken over elements of a partition of the phase space when they are separately used as "holes". Indeed, a "naive" estimate is based on the physical picture that the entire phase space is leaking and thus should average out a slow down of escapes at the periodic points which form a negligible (measure zero) subset of the phase space. However, it was shown numerically in [22] that for the doubling map the opposite inequality holds. Thus, contrary to the seemingly natural expectation based on the rigorous results of [20], it turned out that the naive estimate approaches the average of escape rates from below rather than from above in the limit when the size of the hole tends to zero. It is worthwhile to mention that in this limit both these estimates approach each other.

All elements of a natural Markov partition for the doubling map have the same measures. However, if it is not the case, then other candidates for a naive estimation of the escape rate appear [22]. There was performed a numerical comparison of different naive estimates for the skewed doubling map.

In this chapter, we introduce an estimate for the escape rate, which is applicable for any chaotic dynamical system with generating Markov partition. We prove that the average of escape rates over elements of the partition indeed always exceed a naive estimation of the escape rate. Most importantly, we uncover a reason for the validity of this inequality, i.e. why "escape rate is faster than expected". This reason is the convexity of the logarithm function involved in the definition of the escape rate.

Besides, exact numerical examples are presented for the skewed tent map and Arnold's cat map. We also prove for general maps an inequality between two naive estimates of the escape rate considered in [22] for the skewed doubling map.

## 2.1 Open dynamical systems and escape rate

Assume a map $\hat{T} : \hat{M} \longrightarrow \hat{M}$ generates a dynamical system on the phase space $\hat{M}$ and $H$ be a subset of $\hat{M}$. Then, the open dynamical system corresponding to the map $\hat{T}$ with the hole $H$ is defined by $T : M \longrightarrow \hat{M}$ where $M = \hat{M} \backslash H$ and $T = \hat{T}|_M$. The iterates of $T$ for $k = 1, 2, \ldots$ are defined by $T^k := (\hat{T}|_M)^k$ and we keep track of the iterates of points $x \in M$ as long as they do not enter the "hole" $H$.

For any point $x \in M$, the escape time is defined by the smallest natural number $n$ such that $\hat{T}^n(x) \in H$ and it is denoted by $\tau(x)$. We denote the set of all points that have not escaped after $n$ iterations by

$$M^n = \{x \in M \mid \tau(x) > n\}.$$

It is easy to see that

$$M \supseteq M^1 \supseteq M^2 \supseteq \cdots .$$

Let $\mu$ be a Borel probability measure on $M$. Then upper and lower bounds of the escape rate of the measure $\mu$, respectively, $-\ln \overline{\lambda}$ and $-\ln \underline{\lambda}$ are defined by

$$\ln \overline{\lambda} := \limsup_{n\to\infty} \frac{1}{n} \ln \mu(M^n) \quad and \quad \ln \underline{\lambda} := \liminf_{n\to\infty} \frac{1}{n} \ln \mu(M^n).$$

If $\ln \lambda := \ln \underline{\lambda} = \ln \overline{\lambda}$, then the escape rate of $\mu$ equals $-\ln \lambda$.

Note that we assume $\ln 0 = -\infty$. If $\mu(M^n)$ is well defined, then it is called the survival probability after $n$ iterations. Clearly, the escape rate and survival probability depend on the measure $\mu$. For example, one can choose a Borel measure $\mu$ such that $\mu(M^n) = 0$ for some $n$ or $\mu(M^n) = 1$ for all $n$. If $\hat{T}$ is a measurable map and $H$ is a measurable set with respect to the Borel measure $\mu$, then the escape rate $\rho$ of $\mu$ is defined by,

$$\rho := -\lim_{n\to\infty} \frac{1}{n} \ln \mu(M^n), \tag{2.1}$$

or equivalently,

$$\rho = -\ln(\lim_{n\to\infty} \mu(M^n)^{\frac{1}{n}}). \tag{2.2}$$

when $\lim_{n\to\infty} \mu(M^n)^{\frac{1}{n}} \neq 0$, otherwise $\rho = \infty$.

A Borel measure $\mu$ is called conditionally invariant with respect to $T$ if

$$\mu(A) = \frac{\mu(T^{-1}(A))}{\mu(T^{-1}(M))},$$

for all Borel sets $A \subseteq M$. If $\mu$ is a conditionally invariant measure and $\lambda = \mu(M^1)$, then $-\ln\lambda$ is the escape rate of the open system with respect to the conditionally invariant measure $\mu$.

The following constructive procedure ensures existence of an absolutely continuous conditionally invariant measure (a.c.c.i.m.) for an open dynamical system [15] (an a.c.c.i.m. is a conditionally invariant measure that has density with respect to Lebesgue measure $m$). Assume that $\hat{T} : \hat{M} \longrightarrow \hat{M}$ admits a finite Markov partition $\mathcal{P} = \{E_1, \ldots, E_k\}$ on $\hat{M}$. The existence of Markov partition assumes that $\hat{T}$ is a hyperbolic (i.e. a chaotic) dynamical system because Markov partitions are introduced and exist only for hyperbolic systems. Recall that the dynamical system is called hyperbolic if through almost every points of the phase space are passing stable and unstable manifolds.

Let the hole $H$ be an element of Markov partition $\mathcal{P}$, and $T = \hat{T}|_M$ be the open dynamical system with hole $H$ (i.e. $M = \hat{M}\backslash H$). The (substochastic) transition matrix $P = [p_{ij}]$ of the partition $\mathcal{P}$ under the action of $T$ is defined by

$$p_{ij} = \frac{m(E_i \cap T^{-1}(E_j))}{m(E_i)},$$

where $1 \leq i, j \leq k$ and $m$ is Lebesgue measure. Using refinements of the partition $\mathcal{P}$ given by $\mathcal{P}_n = \bigvee_{i=-n}^{n} \hat{T}^i(\mathcal{P})$, we obtain a sequence of substochastic matrices $P_n$. By Perron-Frobenius theorem, all $P_n$ have a positive leading (i.e. a maximal) eigenvalue $\lambda_n$.

Under the usual conditions of aperiodicity and irreducibility on the matrices $P_n$, there exists an unique probability eigenvector $v_n$ corresponding to $\lambda_n$. If the Markov partition $\mathcal{P}$ is a generating partition, then the sequence of probability eigenvectors $v_n$ will converge to an a.c.c.i.m. $\mu$, where $\mu(M^1) = \lim_{n\to\infty} \lambda_n$. Hence, if we let $\lambda := \mu(M^1) = \lim_{n\to\infty} \lambda_n$, then the escape rate of the open system $T : M \longrightarrow \hat{M}$ with respect to the a.c.c.i.m. $\mu$ is $-\ln \lambda$.

## 2.2 Average of escape rates through elements of a partition is larger than expected

Let $\hat{T} : \hat{M} \longrightarrow \hat{M}$ be a discrete-time dynamical system and $\mu$ be a "natural" invariant probability measure on $\hat{M}$ with respect to $\hat{T}$ (i.e. $\mu(A) = \mu(\hat{T}^{-1}(A))$ for all Borel sets $A \subseteq \hat{M}$). We also assume that the "closed" dynamics is ergodic with respect to $\mu$. The assumption of ergodicity ensures that almost all (i.e. measure one subset) orbits will eventually enter a "hole" when the hole is a subset of positive measure of the phase space. We assume for simplicity that $\mu$ is absolutely continuous (i.e. has a density) with respect to Lebesgue measure.

Consider a Markov partition $\{E_1, \ldots, E_k\}$ of the phase space $\hat{M}$ with elements $E_i$ of positive measures (i.e. $\mu(E_i) > 0$ for all $i$). Let $T_i = \hat{T}|_{\hat{M}\setminus E_i}$ be the open dynamical system with hole $E_i$. We assume $T_i$ admits an a.c.c.i.m. $\mu_i$ such that its escape rate $\rho_i$ is well-defined. We also denote the set of all points that have not escaped after $n$ iterations of $T_i$ by $M_i^n$. That means,

$$M_i^n := \{x \in \hat{M}\setminus E_i \mid \tau_i(x) > n\},$$

where $\tau_i(x)$ is the escape time of the open dynamical system $T_i$. Moreover, we assume that $T_i$ is a measurable map and $E_i$ is a measurable set with respect to the a.c.c.i.m. $\mu_i$. Under these assumptions for all $i = 1, \ldots, k$, we can set

$$p_i := \mu_i(M_i^1) = \lim_{n\to\infty} (\mu_i(M_i^n))^{1/n}. \tag{2.3}$$

**Proposition 2.2.1.** *Let $\hat{T} : (\hat{M}, \mu) \longrightarrow (\hat{M}, \mu)$ be a probability measure preserving discrete-time dynamical system such that there is a finite Markov partition $\mathcal{P} = \{E_1, \ldots, E_k\}$ with elements $E_i$ of positive measures. If all open dynamical systems $T_i = \hat{T}|_{\hat{M}\setminus E_i}$ admit an a.c.c.i.m., then*

$$\langle \rho \rangle := \sum_{i=1}^{k} \mu(E_i)\rho_i \geq -\ln(\sum_{i=1}^{k} \mu(E_i)p_i). \tag{2.4}$$

*Proof.* If $p_i \neq 0$ for all $i = 1, \ldots, k$, then by making use of (2.2), we obtain

$$\langle \rho \rangle = \sum_{i=1}^{k} \mu(E_i)\rho_i = -\sum_{i=1}^{k} \mu(E_i)\ln(p_i).$$

Because $-\ln(x)$ is a convex function, the relation (2.4) follows from Jensen's inequality. Moreover, if $p_i = 0$ for some $1 \leq i \leq k$, then $\rho_i = \infty$, and it is easy to see that (2.4) is satisfied in this case as well. □

The left side of (2.4) is the average (with respect to the invariant probability measure $\mu$) of escape rates over all positions of the hole, i.e. over all elements of the Markov partition. The right-hand side of (2.4) is equivalent to the escape rate of the system when we consider uniform density with a uniform leak from it where the hole's size is equal to the average of $1-\mu_i(M_i^1)$, $1 \leq i \leq k$, with respect to the probability measure $\mu$. Under these assumptions, the estimate of escape rate is

$$-\ln(1 - \sum_{i=1}^{k} \mu(E_i)(1 - \mu_i(M_i^1))). \tag{2.5}$$

Then, (2.3) and (2.5) imply

$$-\ln(1 - \sum_{i=1}^{k} \mu(E_i)(1 - \mu_i(M_i^1))) = -\ln(\sum_{i=1}^{k} \mu(E_i)\mu_i(M_i^1)) = -\ln(\sum_{i=1}^{k} \mu(E_i)p_i). \tag{2.6}$$

Hence, (2.4) and (2.6) show that the (average) escape rate is faster than the estimate of escape rates when we assume that the density remains uniform in the system and the hole's

size is the average of $1-\mu_i(M_i^1)$ with respect to the probability measure $\mu$. Remind that at each iteration of the map $T_i$ the same portion $1-\mu_i(M_i^1)$ of the remaining in the phase space points escapes through the hole $E_i$ with respect to the a.c.c.i.m. $\mu_i$. Therefore, the average of $1-\mu_i(M_i^1)$ is the average on proportional leaks of open systems $T_i$ with respect to their a.c.c.i.m. $\mu_i$.

There are some other candidates for (naive) estimation of the escape rate based on the physical picture of uniform leaking in the whole phase space (see e.g. [22]). The first one is $-\ln(1-h)$ where $h=1/k$ is the average of holes' sizes (i.e. $h=\frac{\sum_{i=1}^{k}\mu(E_i)}{k}$) and $k$ is the number of elements in a Markov partition. We will denote this naive estimation with $N_1$. This naive estimate comes from the assumption that the density of the a.c.c.i.m. remains uniform in the system and the hole's size is equal to $h=1/k$.

The second candidate $N_2$ for a naive estimate of the escape rate was introduced in [22]. It is defined as $N_2 := -\sum_{i=1}^{k} h_i \ln(1-h_i)$ where $h_i=\mu(E_i)$ (Recall that $\mu$ is the invariant probability measure of the corresponding closed system). The naive estimate $N_2$ uses the assumption that the density of conditionally invariant measure is a constant in a complement of a corresponding hole. The estimate of escape rate of open system with hole $E_i$ is $-\ln(1-h_i)$ where $h_i=\mu(E_i)$. Then, $N_2$ is the average of these estimates over different positions of the hole in the phase space (over the elements of Markov partition) with respect to probability measure $\mu$.

By making use of the Jensen's inequality, we obtain

$$N_2=-\sum_{i=1}^{k} h_i \ln(1-h_i) \geq -\ln(\sum_{i=1}^{k} h_i(1-h_i)) = -\ln(1-\sum_{i=1}^{k} h_i^2). \qquad (2.7)$$

It is easy to see that

$$\sum_{i=1}^{k} h_i^2 \geq h=\frac{1}{k}, \qquad (2.8)$$

since $1 = \sum_{i=1}^{k} \mu(E_i) = \sum_{i=1}^{k} h_i$. Then, (2.7) and (2.8) imply

$$N_2 \geq -\ln(1 - \sum_{i=1}^{k} h_i^2) \geq -\ln(1-h) = N_1.$$

Therefore, the naive estimation $N_2$ is greater than or equal to $N_1$. These two naive estimates become equal only if elements of the partition have equal sizes (i.e. $\mu(E_i) = 1/k$ for all $i$).

## 2.3 Examples

### 2.3.1 Skewed tent map

Consider a skewed tent map $T : [0,1] \longrightarrow [0,1]$ given by:

$$T(x) = \begin{cases} \dfrac{x}{x_0} & x \in [0, x_0), \\ \dfrac{1-x}{1-x_0} & x \in [x_0, 1], \end{cases} \tag{2.9}$$

where $x_0 \in (0,1)$. Consider a Markov partition $\mathcal{E} = \{E_1, E_2\}$ of the phase space $[0,1]$, where $E_1 = [0, x_0]$ and $E_2 = [x_0, 1]$. Let $\rho_i$ denote the escape rate of the open system with hole $E_i$. By making use of (2.1) or (2.2), we obtain

$$\rho_1 = -\ln(1-x_0), \qquad\qquad \rho_2 = -\ln(x_0).$$

Thus,

$$\langle \rho \rangle := m(E_1)\rho_1 + m(E_2)\rho_2 = -x_0 \ln(1-x_0) - (1-x_0)\ln(x_0), \tag{2.10}$$

where $m$ is Lebesgue measure (the natural invariant probability measure of (2.9)). From (2.3), we get $p_1 = 1 - x_0$ and $p_2 = x_0$. Then,

$$-\ln(\sum_{i=1}^{2} m(E_i)p_i) = -\ln(2x_0(1-x_0)). \tag{2.11}$$

From (2.10) and (2.11) by using Jensen's inequality, we obtain

$$\langle \rho \rangle \geq -\ln(\sum_{i=1}^{2} m(E_i)p_i). \tag{2.12}$$

If $x_0 = \frac{1}{2}$, then the equality will be satisfied in (2.12).

We compare now our estimate of the escape rate which is the lower bound (right-hand side) of the inequality (2.4) with the naive estimate $N_1 = -\ln(1-h)$ of the escape rate, where $h$ is the average of holes' (elements of partition) sizes [16, 22]. To do this we consider refinements of the partition $\mathcal{E} = \{[0, x_0], [x_0, 1]\}$ under the skewed tent map $T$ to construct Markov partitions with $4,\ 8, \ldots,\ 128$, or $256$ elements.

The Table 2.1 presents values of our estimation of escape rates of the skewed tent map (2.9), where $x_0 = 0.1,\ 0.2,\ 0.3,\ 0.4$, or $0.5$ and the partition has $4,\ 8, \ldots,\ 128$, or $256$ elements. In Table 2.2, naive estimations $N_1$ of the skewed tent map are presented, where the partition has $4,\ 8, \ldots,\ 128$, or $256$ elements. We know $N_1$ only depends on the number of elements in a partition, and it does not depend on the size of holes.

Table 2.1: The values of the right-hand side of (2.4) for the skewed tent map, where $x_0 = 0.1,\ 0.2,\ 0.3,\ 0.4$, or $0.5$ and the partition has $4,\ 8, \ldots,\ 128$, or $256$ elements.

| | 4 | 8 | 16 | 32 | 64 | 128 | 256 |
|---|---|---|---|---|---|---|---|
| 0.1 | 0.77922 | 0.44239 | 0.28375 | 0.19638 | 0.14384 | 0.10949 | 0.08598 |
| 0.2 | 0.47400 | 0.25981 | 0.16685 | 0.11452 | 0.07286 | 0.04757 | 0.03175 |
| 0.3 | 0.37517 | 0.21720 | 0.11717 | 0.06234 | 0.03491 | 0.01987 | 0.01149 |
| 0.4 | 0.37047 | 0.17868 | 0.08023 | 0.03931 | 0.01990 | 0.01022 | 0.00529 |
| 0.5 | 0.42387 | 0.15808 | 0.06928 | 0.03297 | 0.01604 | 0.00792 | 0.00393 |

Table 2.2: The naive estimation $N_1$ of the escape rate of the skewed tent map, where the partition has $4,\ 8, \ldots,\ 128$, or $256$ elements.

| | 4 | 8 | 16 | 32 | 64 | 128 | 256 |
|---|---|---|---|---|---|---|---|
| $N_1$ | 0.28768 | 0.13353 | 0.06453 | 0.03174 | 0.01574 | 0.00784 | 0.00391 |

Comparing the data of Table 2.1 with Table 2.2, one can see our estimation of the escape

rate is greater than the naive estimation $N_1$ for the skewed tent map.

### 2.3.2 Arnold's cat map

Let $\mathbb{T}^2$ be a torus, i.e the unit square $\mathbf{S} = [0,1] \times [0,1]$ with standard identification of its opposite sides. The Arnold's cat map $T : \mathbb{T}^2 \longrightarrow \mathbb{T}^2$ is defined by

$$T(\begin{bmatrix} x \\ y \end{bmatrix}) = \begin{bmatrix} 2 & 1 \\ 1 & 1 \end{bmatrix} \begin{bmatrix} x \\ y \end{bmatrix} \mod 1.$$

The eigenvalues of $\begin{bmatrix} 2 & 1 \\ 1 & 1 \end{bmatrix}$ are $\lambda_1 = \frac{3+\sqrt{5}}{2}$ and $\lambda_2 = \frac{3-\sqrt{5}}{2}$, where

$$v_1 = \begin{bmatrix} 1 \\ \frac{\sqrt{5}-1}{2} \end{bmatrix}, \quad v_2 = \begin{bmatrix} 1 \\ -\frac{\sqrt{5}+1}{2} \end{bmatrix},$$

are their corresponding eigenvectors, respectively.

It is easy to see that this map preserves the Lebesgue measure (area) on the torus (it is the natural invariant probability measure of Arnold's cat map). Consider rectangles $ABCD$ and $DEFG$ where their sides are parallel to the directions of eigenvectors $v_1$ and $v_2$ (as it is shown in Fig. 2.1). Take now the partition $\{R_1, R_2\}$ of $\mathbb{T}^2$, where $R_1$ ($R_2$) is the projection of rectangle $ABCD$ ($DEFG$) on the torus $\mathbb{T}^2$. Recall that the plane is a natural unfolding of the torus under identification of its parallel sides.

The partition $\{R_1, R_2\}$ is not a generating one, but one can build the generating partition

$\mathcal{L} = \{L_1, L_2, L_3, L_4, L_5\}$ from $\{R_1, R_2\}$ as follows [25]:

$$L_1 \cup L_3 = R_1 \cap T(R_1),$$
$$L_2 = R_1 \cap T(R_2),$$
$$L_4 = R_2 \cap T(R_1),$$
$$L_5 = R_2 \cap T(R_2).$$

See Fig. 2.1 for more details.

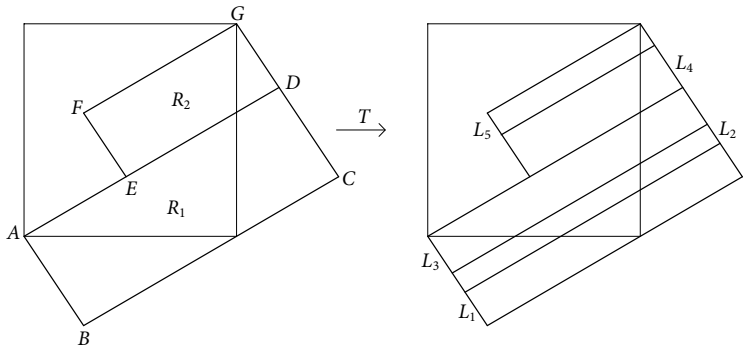


Figure 2.1: $B = (\frac{\sqrt{5}-1}{2\sqrt{5}}, \frac{-1}{\sqrt{5}})$, $C = (\frac{\sqrt{5}+1}{\sqrt{5}}, \frac{\sqrt{5}-1}{2\sqrt{5}})$, $D = (\frac{\sqrt{5}+3}{2\sqrt{5}}, \frac{\sqrt{5}+1}{2\sqrt{5}})$, $E = (\frac{1}{\sqrt{5}}, \frac{\sqrt{5}-1}{2\sqrt{5}})$, $F = (\frac{\sqrt{5}-1}{2\sqrt{5}}, \frac{\sqrt{5}-1}{\sqrt{5}})$.

Let $T_0$ be the transition probability matrix of the partition $\mathcal{L}$ under the map $T$, then

$$T_0 = \begin{bmatrix} \frac{3-\sqrt{5}}{2} & 0 & \frac{3-\sqrt{5}}{2} & \sqrt{5}-2 & 0 \\ \frac{3-\sqrt{5}}{2} & 0 & \frac{3-\sqrt{5}}{2} & \sqrt{5}-2 & 0 \\ \frac{3-\sqrt{5}}{2} & 0 & \frac{3-\sqrt{5}}{2} & \sqrt{5}-2 & 0 \\ 0 & \frac{\sqrt{5}-1}{2} & 0 & 0 & \frac{3-\sqrt{5}}{2} \\ 0 & \frac{\sqrt{5}-1}{2} & 0 & 0 & \frac{3-\sqrt{5}}{2} \end{bmatrix}.$$

Consider the open dynamical system built from Arnold's cat map with the hole $L_i$. If we denote the substochastic matrix of transition probabilities of this open system by $T_i$, then $T_i$ is equal to $T_0$ where the $i$th row of $T_0$ is replaced by zeros.

Let $\mathcal{L}_n = \bigvee_{i=-n}^{n} T^i(\mathcal{L})$ denote the refinements of partition $\mathcal{L}$ under the action of the map $T$ and $T_{i,n}$ be the substochastic transition matrix corresponding to the refined partition $\mathcal{L}_n$ of the open dynamical system with hole $L_i$. It is easy to check that $T_{i,n}$ and $T_i$ for all $n = 1, 2, \ldots$ have the same leading eigenvalues $\lambda_i$. Also, we know $\mathcal{L}$ is a generating Markov partition and all $T_{i,n}$ satisfy aperiodicity and irreducibility conditions. Therefore, there is an a.c.c.i.m. $\mu_i$ where the escape rate of the open system with hole $L_i$ with respect to $\mu_i$ is $-\ln \lambda_i$. Here, we have

$$\lambda_1 = \lambda_2 = \lambda_3 = \lambda_4 = 3 - \sqrt{5}, \quad \lambda_5 = \frac{1+\sqrt{2}}{2}(3 - \sqrt{5}).$$

Hence, the escape rates corresponding to the a.c.c.i. measures $\mu_i$ are

$$\rho_1 = \rho_2 = \rho_3 = \rho_4 = -\ln(3 - \sqrt{5}), \quad \rho_5 = -\ln(\frac{1+\sqrt{2}}{2}(3 - \sqrt{5})).$$

Thus, the average of escape rates with respect to Lebesgue measure is

$$\langle \rho \rangle = \sum_{i=1}^{5} m(L_i)\rho_i \simeq 0.2494, \tag{2.13}$$

where

$$\begin{aligned}
m(L_1) = m(L_3) &= \frac{3-\sqrt{5}}{2}\sqrt{\frac{\sqrt{5}+3}{10}}, \\
m(L_2) &= (\sqrt{5}-2)\sqrt{\frac{\sqrt{5}+3}{10}}, \\
m(L_4) &= \frac{\sqrt{5}-1}{2}\left(1 - \sqrt{\frac{\sqrt{5}+3}{10}}\right), \\
m(L_5) &= \frac{3-\sqrt{5}}{2}\left(1 - \sqrt{\frac{\sqrt{5}+3}{10}}\right).
\end{aligned}$$

From (2.3), we obtain $p_1 = p_2 = p_3 = p_4 = \lambda_1 = 3 - \sqrt{5}$ and $p_5 = \lambda_5 = \frac{1+\sqrt{2}}{2}(3 - \sqrt{5})$.

Therefore,

$$-\ln(\sum_{i=1}^{5} m(L_i)p_i) \simeq 0.2476. \tag{2.14}$$

By comparing (2.13) and (2.14), we see that the average of escape rates over the elements of Markov partition $\mathcal{L}$ is greater than the estimation of escape rate for the Arnold's cat map.

### 2.3.3 The Ulam-von Neumann logistic map

There are only a few examples of nonlinear systems where the escape rate is studied. Consider the nonlinear Ulam$-$von Neumann map of the unit interval [26],

$$T(x) = 4x(1-x), \qquad x \in [0,1]. \tag{2.15}$$

It is well-known that this map is metrically conjugate to the tent map (defined by (2.9) when $x_0 = \frac{1}{2}$), where the conjugate map $U$ is given by,

$$U(x) = \sin^2(\frac{\pi x}{2}).$$

The invariant probability measure $\mu$ of Ulam$-$von Neumann logistic map (2.15) has non-uniform density $f(x)$ with respect to Lebesgue measure $m$, where

$$f(x) = \frac{1}{\pi\sqrt{x(1-x)}}.$$

We consider the following Markov partition on the unit interval of the logistic map,

$$\mathcal{P} = \left\{ P_i \mid P_i = \left[ \sin^2\left(\frac{i\pi}{2^{n+1}}\right), \sin^2\left(\frac{(i+1)\pi}{2^{n+1}}\right) \right],\ i = 0,1,2,\ldots,2^n-1 \right\},$$

where the partition $\mathcal{P}$ is the image of the natural Markov partition

$$\mathcal{E} = \left\{ E_i \mid E_i = \left[ \frac{i}{2^n}, \frac{i+1}{2^n} \right],\ i = 0,1,2,\ldots,2^n-1 \right\},$$

of tent map under the conjugate map $U(x)$. It is easy to see that $\mu(P_i) = m(E_i) = \frac{1}{2^n}$ for all $i = 0, 1, \ldots, 2^n - 1$. Moreover, the transition probability matrix of the partition $\mathcal{P}$ under Ulam−von Neumann logistic map is the same as the transition matrix of the tent map for the partition $\mathcal{E}$. These two maps also have the same transition matrices on the corresponding refinements of their partitions.

Let $T_i$ denote the open dynamical system of the logistic map with hole $P_i$. Clearly, $T_i$ will have the same substochastic transition matrices as the open tent map with hole $E_i$ on refinements of their corresponding Markov partitions. Hence, the escape rate $\rho_{T_i}$ of $T_i$ is equal to the escape rate $\rho_i$ of open tent map with hole $E_i$. It implies

$$\sum_{i=0}^{2^n-1} \mu(P_i)\rho_{T_i} = \sum_{i=0}^{2^n-1} m(E_i)\rho_i.$$

For the same reason as before, the lower bound (the right-hand side) of the inequality (2.4) (i.e. our naive estimate of the escape rate) will be the same for both these systems. Thus, the relation between our estimate of the escape rate (lower bound of (2.4)) and the naive estimate $N_1$ will be valid in this case as well (see Tables 2.1 and 2.2).

## 2.4 Concluding remarks

We have shown that for chaotic maps which admit a finite generating Markov partition, the averaged over the elements of the Markov partition escape rate exceed a naive estimate of the escape rate.

A natural question would be to analyze relations between these and other possible estimates of a global (average) escape rate in nonlinear dynamical systems. We believe that our argument based on convexity will be still an important basic tool in this case as well.

A standard approach going back to Sinai is to consider a sequence of Markov partitions with smaller and smaller elements [27]. Then the map becomes closer and closer to a linear on the elements of Markov partitions, and thus the entire dynamical system is approximated

by a sequence of Markov chains. To perform such proofs, it seems that the higher (second) order approximation for escape rate in terms of the size of a "hole" obtained in [22] could be quite useful. It is also worthwhile to mention in this respect that it was observed numerically [28] that in (nonlinear) logistic maps the process of escape also slows down near periodic orbits.

There is also a direct connection between Markov chains, dynamical systems with Markov partitions, and transport (dynamics) on networks [29, 30]. Namely, the adjacency matrix of a network (which has the entry $1$ if the element $i$ is connected by an edge to the element $j$, or otherwise $0$ entries), can always be considered as a structural matrix of a Markov chain or as a transition matrix of a topological Markov chain (directed graph). Therefore, the results about open Markov systems are applicable to networks with leaking elements and allow for estimates of average leaking, most leaking sites, etc [30, 31].

# CHAPTER 3
# COLLISION OF A HARD BALL WITH SINGULAR POINTS OF THE BOUNDARY

As it was mentioned, when we replace the point particle with a physical particle (disc), then dynamics may drastically change. Namely, any type of transition from regular to chaotic dynamics may occur, and vice versa. Moreover, these transitions may occur as soft (i.e. for any positive radius of the moving ball) as well as hard ones (i.e. for sufficiently large balls). All these transitions can occur in the presence of singularities in the boundary of a billiard table. Here, we describe which types of singularities may result in a change of dynamics in transition from a point particle to a hard ball. We also discuss possible types of collisions of a hard ball with a point, which are consistent with the laws of mechanics. It is shown that the collision law for a smooth hard ball, used so far in the studies of physical billiards, is indeed consistent (satisfies) to mechanical conservation laws respected by collisions. It is also shown that a rough ball collision law, when a ball acquires rotation after a collision, is also consistent with the laws of mechanics.

It is worthwhile to mention that the most celebrated billiard system is a gas of hard balls (Boltzmann gas) where moving particles are indeed hard balls. However, this system can be reduced to a mathematical billiard within a billiard table with a specific boundary. In fact, studies of dynamics of the Boltzmann gas inspired Ya. G. Sinai to introduced famous Sinai billiards, which made the foundation for the theory of chaotic billiards. However, the dynamics of Sinai billiards and other most famous mathematical billiards does not change after the transition to physical billiards in the same billiards tables. In fact, changes in dynamics occur only when the boundary of a billiard table has a visible singularity, i.e. a point in the intersection of two or more smooth components of the boundary such that a small enough physical particle can hit that point of the boundary. If a billiard table is two-

dimensional, then such singularities are internal corners where two smooth components of the boundary intersect and make an angle greater than $\pi$ inside the billiard table. In all papers cited above, it was assumed that reflection of the ball off such visible singularity occurs in a natural manner corresponding to the simplest elastic collision. In the present note, we justify this assumption for a smooth hard ball. It is worthwhile to mention that there are other types of reflection of a ball off a visible singular point that correspond to a rough ball which may acquire rotation after such collision [32] even under the assumption that it is a no-slip collision [33, 34]. We demonstrate that both types of reflection, for a smooth ball and a hard ball, satisfy the (conservation) laws of mechanics. Therefore physical billiards generated by the motion of a smooth or a rough ball can be considered as natural realistic dynamical systems.

### 3.1 Different types of boundary singularities in billiard tables

Let $Q$ be a domain in $d$-dimensional Euclidean space $\mathbf{R}^d$ such that its boundary $\partial Q$ is the union of a finite number of $C^1$-smooth $(d-1)$-dimensional manifolds. A point $q$ of the boundary $\partial Q$ is called singular if the boundary is not differentiable at that point. That means a singular point belongs to the intersection of some (at least two) differentiable (aka regular) components of the boundary. Note that we also call a singular point in dimension two (i.e. $\dim Q = 2$) a corner. All non-singular points of the boundary $\partial Q$ are called regular points.

Consider a free motion of a hard ball (a disk in $\dim 2$) of radius $r > 0$ in the domain $Q$ with elastic reflections off the boundary $\partial Q$. The resulting dynamical system is called a physical billiard [10], and the domain $Q$, a billiard table. To describe the dynamics of such ball, it is enough to follow the motion of its center. It is easy to see that the center of the ball moves in the smaller billiard table, which one gets by moving any point $q$ of the boundary by $r$ to the interior of the billiard table along the internal unit normal vector $n(q)$ [10].

We will call a singular point $q$ of the boundary $\partial Q$ an invisible singular point if for any $r > 0$ the hard ball of radius $r$ cannot hit that point. Otherwise, a singular point is called a visible singular point. Therefore, $q$ is a visible singular point of a billiard table if a ball with a sufficiently small radius can hit $q$. A formal mathematical definition of a visible singular point (in any dimension) is the following one. A singular point $A$ is a visible singular point if for any neighborhood $N$ of $A$ the convex hull of $Q \cap N$ contains a neighborhood of $A$.

We also call a visible singular point in dimension two an internal corner. For example, Fig. 3.1 shows visible and invisible singular points in dimension two.

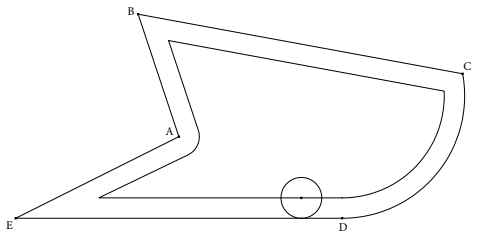


Figure 3.1: Corners (singular points) B, C, and E are invisible to any disk. The point D is not singular, since boundary is differentiable at D. The corner A is an internal corner (a visible singular point).

Note that being a visible singular point (an internal corner) does not mean that a hard ball of any radius $r > 0$ can reach (hit) that point. Namely, if the radius of the particle is larger than some constant (which depends on the shape of a billiard table), then some visible singular points become invisible (see Fig. 3.2).

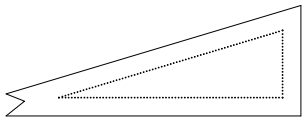

Figure 3.2: An internal corner becomes invisible when radius of disk is larger than some constant.

Observe that at the moment of collision with a visible singular point, the center of hard ball can be at different positions, and these possible positions depend on the shape of the

boundary $\partial Q$ (see Fig. 3.3). This should be contrasted with the collision of the ball off the boundary at a regular point, when the center of the ball always has one position, namely at the distance $r$ on the internal normal line to the boundary of a billiard table. In Fig. 3.3, two situations are depicted, which may happen in three dimensional billiard tables.

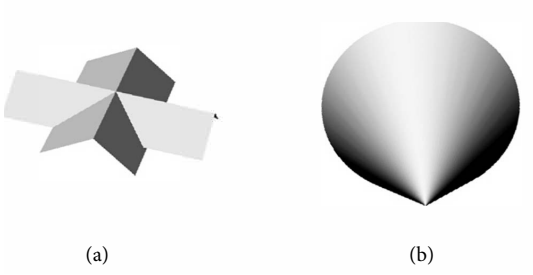


Figure 3.3: (a) There are two lines of visible singular points. When a hard ball hits a point on those lines, its center is on an arc of a circle centered at that point and orthogonal to the corresponding line. However, at the moment of collision with the intersection point of those two lines the center of hard ball can be only in one position. (b) Here is one isolated visible singular point. At the moment of collision with such singularity the center of a hard ball is on a piece of 2-sphere centered at that singular point.

Since the particle is a hard ball, it will keep its shape at the moment of collision. Hence the center of the hard ball is at the distance $r$ from a collision point (regardless of whether this point is a regular or singular point of the boundary). Therefore, the boundary of the reduced billiard table of the mathematical billiard, which has the same dynamics as the considered physical billiard [10], acquires a piece of a sphere (or an arc of a circle if the dimension of the billiard table is two) of radius $r$ with the center at the visible singular point. Hence the reduced billiard table of the equivalent mathematical billiard has a dispersing component in the boundary which generates a chaotic (hyperbolic) dynamics in case if a moving particle is a hard ball.

In 3.4, it is easy to see the boundary of the reduced billiard table of the mathematical billiard acquires a dispersing component, because of the case of dimension two depicted. Here, the center of a disk can be located at any point of an arc of the circle with the center at the singular point and with the radius equals to the radius of the disk.

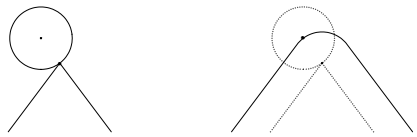

Figure 3.4: A collision between a disk and a visible singular point (here, an internal corner) is shown in the left picture. On the right, one can see its equivalent for a (virtual) collision between disk's center and an arc of a circle centered at the internal corner with the same radius as the disk's radius.

The fact that a reduced billiard table of the equivalent mathematical billiard acquires a dispersing (or semi-dispersing) component holds true for any type of collision of the physical ($r > 0$) particle with the boundary at a visible singular point. However, such collisions can generally be elastic or inelastic (i.e. angle of incident is equal to the angle of reflection or not) and with or without slip (i.e. collision occurs at a point of the boundary or the particle slip on the boundary) [32, 34]. Dynamics of rough ball even in case of no-slip collisions is much more complicated than the dynamics of a smooth ball.

It is also worthwhile to mention that if a billiard table has an internal visible corner, in the transition from mathematical to a physical billiard, the boundary of a reduced billiard table becomes smoother than the boundary of the initial billiard table. Indeed, instead of a corner appears an arc of a circle that has common tangents with neighboring components of the boundary. However, this smoothening does not influence the dynamics. Dynamics gets changed because of the appearance of a (new) dispersing component of the boundary, which makes it more chaotic.

### 3.2 No-slip collisions of a hard ball with a visible singular point

In the case of no-slip collisions, each reflection of the moving particle (hard ball) off the boundary occurs at a single point. Hence a collision at any point of the boundary does not depend on the shape of the boundary elsewhere. Therefore, the collision problem can be actually considered as a reflection of a hard ball off a point.

At the moment of the collision, the impulse $\Delta P$ decomposes into two components, which are the normal impulse $\Delta P_N$ acting towards the center of hard ball and the tangent impulse $\Delta P_T$ based on friction which is tangent to the hard ball at the collision point. The tangent impulse can result in either loss of kinetic energy or exchange between linear and angular momentum while the total kinetic energy is preserved. We will consider the friction-free (elastic) collision and the case when the impulse $\Delta P_T$ results in an exchange between linear and angular momentum without loss of energy. In other words, we consider only conservative (Hamiltonian) dynamics.

Let a hard ball of radius $r > 0$ with the center at a point $O$ hits a visible singular point $A$ of the boundary of a billiard table $Q$. Without any loss of generality we assume that the mass of the hard ball is $m = 1$. Denote the linear velocity of hard ball's center just before (after) the collision by $V^b$ ($V^a$). Consider now a decomposition of $V^b$ to two components $V_N^b$ and $V_T^b$, where $V_N^b = Proj_{\overrightarrow{OA}} V^b$ and $V_T^b = V^b - V_N^b$. Note that we will use the superscript $a$ instead of $b$ to denote velocity components at a moment of time right after the reflection. Denote also the vector form of angular velocity just before (after) the collision about the point $O$ by $\omega^b$ ($\omega^a$).

The collision map $S$ at point $A$ will map linear components and the angular component of the velocity just before collision $(V_N^b, V_T^b, \omega^b)$ to those right after collision $(V_N^a, V_T^a, \omega^a)$. The map $S$ has the following properties:

1. The map $S$ is an orthogonal map because of the assumption that the system in question is Hamiltonian.

2. Because of time reversibility of dynamics, $S^2$ is the identity map.

3. The normal component of the linear velocity with respect to the boundary of hard ball at the contact point $A$ (i.e. $V_N^b$) always reverses under the map $S$.

The conditions 1 and 2 imply that the eigenvalues of the map $S$ are $1$ or $-1$. In view of 3, one gets $S(V_N^b, V_T^b, \omega^b) = (-V_N^b, V_T^a, \omega^a)$, or equivalently, $V = (V_N^b, \vec{0}, \vec{0})$ is an eigenvector

of $S$ corresponding to the eigenvalue $-1$. It also implies that $\Delta P_N = -2V_N^b$.

The Hamiltonian system under consideration satisfies three conservation laws of the kinetic energy $K$, the linear momentum $P$, and the angular momentum $L$ about the point $O$. These conservation laws in dimension 3 are given by the relations

$$\begin{cases} K^b = \frac{1}{2}\left(|V_N^b|^2 + |V_T^b|^2 + I|\omega^b|^2\right) \\ \quad = \frac{1}{2}\left(|V_N^a|^2 + |V_T^a|^2 + I|\omega^a|^2\right) = K^a, \\ P^b + \Delta P = V_N^b + V_T^b + \Delta P_N + \Delta P_T = V_N^a + V_T^a = P^a \\ L^b + \Delta P_T \times \overrightarrow{AO} = I\omega^b + \Delta P_T \times \overrightarrow{AO} = I\omega^a = L^a, \end{cases} \tag{3.1}$$

where $I$ is the moment of inertia of the hard ball.

Using that $V_N^a = -V_N^b$ and $\Delta P_N = -2V_N^b$, one can simplify (3.1) as

$$\begin{cases} |V_T^b|^2 + I|\omega^b|^2 = |V_T^a|^2 + I|\omega^a|^2, \\ V_T^b + \Delta P_T = V_T^a \\ I\omega^b + \Delta P_T \times \overrightarrow{AO} = I\omega^a. \end{cases} \tag{3.2}$$

In the following, we consider two cases about the impulse $\Delta P_T$: friction-free collision (i.e. $\Delta P_T = \vec{0}$), and collisions with friction (i.e. $\Delta P_T \neq \vec{0}$). By solving (3.2) for $\Delta P_T$, we get

$$\langle \Delta P_T, \frac{r^2 + I}{I}\Delta P_T + 2V_T^b + 2\overrightarrow{AO} \times \omega^b \rangle = 0, \tag{3.3}$$

where $\langle ., . \rangle$ is the inner product in $\mathbf{R}^3$ and $r$ is radius of hard ball.

Observe that the conservation laws in dimension 2 are the same as in (3.1) under the assumption that the billiard table $Q$ is a subset of $xy$-plane in $\mathbf{R}^3$.

### 3.2.1 Friction-free collision (a smooth ball)

In this section, we study a friction-free (i.e. $\Delta P_T = \vec{0}$) Hamiltonian system. In this case, (3.2) implies

$$V_T^a = V_T^b, \qquad \omega^a = \omega^b.$$

Here, the solution $(V_N^a, V_T^a, \omega^a) = (-V_N^b, V_T^b, \omega^b)$ of (3.1) corresponds to the case of smooth hard ball [32] when the ball does not acquire rotation upon collision. Thus, in this case, we have an elastic reflection where the angle of incidence is equal to the angle of reflection.

Also, this friction-free collision is equivalent to the elastic reflection of the hard ball's center $O$ off a piece of a 2-sphere (it can be an arc of a circle) centered at the visible singular point $A$ with the same radius as the radius of the hard ball [10, 11].

In case of dimension 3, the collision map $S$ is a linear map from a 6-dimensional subspace of $\mathbf{R}^9$ to itself with eigenvalues 1 and $-1$. When $\Delta P_T = \vec{0}$, the eigenvectors which correspond to these eigenvalues have the forms $(\vec{0}, V_T^b, \omega^b)$ and $(c\overrightarrow{AO}, \vec{0}, \vec{0})$, respectively, where $c$ is a constant. Also, the eigenspaces corresponding to the eigenvalues 1 and $-1$ have dimensions five and one, respectively.

### 3.2.2 Collisions with friction (a rough ball)

For the Hamiltonian system under consideration, the presence of the frictional force means that $|\Delta P_T| \neq 0$. The corresponding solution of (3.1) when $|\Delta P_T| \neq 0$ describes the dynamics of a rough ball [32], which has no-slip ultra-elastic reflections off the boundary (After an ultra-elastic reflection, the ball will acquire rotation, therefore, the incident angle is not equal to the reflection angle [32]). In this case, the tangential component of the linear velocity partially transfers to the angular velocity and vice versa.

A nontrivial solution for $\Delta P_T$ in (3.3), is given by

$$\Delta P_T = -\frac{2I}{r^2 + I}(V_T^b + \overrightarrow{AO} \times \omega^b). \tag{3.4}$$

Let $S$ be the collision map in dimension 3 when the tangent impulse $\Delta P_T$ is given by (3.4). Then $(\vec{0}, V_T^b, \omega^b)$ is an eigenvector of the collision map $S$ corresponding to the eigenvalue 1 if $V_T^b + \overrightarrow{AO} \times \omega^b = \vec{0}$. The solution set of the vector equation $V_T^b + \overrightarrow{AO} \times \omega^b = \vec{0}$ is a three dimensional space. Hence, the eigenspace corresponding to the eigenvalue 1 of the collision map $S$ is a 3-dimensional space.

Moreover, $(\vec{0}, V_T^b, \omega^b)$ is an eigenvector of the collision map $S$ which corresponds to the eigenvalue $-1$ if $V_T^b \times \overrightarrow{AO} - I\omega^b = \vec{0}$. In this case, the solution set of the vector equation $V_T^b \times \overrightarrow{AO} - I\omega^b = \vec{0}$ is a two dimensional space. This implies that the eigenspace corresponding to the eigenvalue $-1$ of the collision map $S$ is a 3-dimensional space (we know $(\overrightarrow{AO}, \vec{0}, \vec{0})$ is another eigenvector for eigenvalue $-1$).

# CHAPTER 4

# EHRENFESTS' WIND-TREE MODEL IS DYNAMICALLY RICHER THAN THE LORENTZ GAS

The Ehrenfests' Wind-Tree model was introduced in the celebrated paper by Paul and Tatyana Ehrenfest [35] as a simple mechanical (dynamical) model for diffusion. In their model scatterers were rhombuses and this system itself was called a Wind-Tree model, where "wind" stays for the particle and "tree" for a scatterer [35]. The Wind-Tree model was extensively studied by physicists [4, 5, 6, 36, 37, 38].

It turned out that this system is not a good model for diffusion. Indeed the Wind-Tree model is a billiard dynamical system and, because the boundary of the corresponding billiard table consists of straight segments, its dynamics is similar to billiards in polygons. It is well known that billiards in polygons have zero Kolmogorov-Sinai entropy and cannot generate dynamical chaos which is a necessary condition for demonstrating stochastic behavior and, in particular, diffusion. The Wind-Tree model was actively studied in statistical mechanics after appearance of powerful computers and found lacking of diffusion [5, 6, 38, 39, 40]. Instead, the role of the basic simplest mechanical model of diffusion was very successfully played by the celebrated Lorentz gas where the scatterers are circles rather than rhombuses [41, 42, 43]. Therefore these billiard systems belong to the class of the most chaotic billiards. In fact, Lorentz gas is unfolding of a Sinai billiard [3]. Notably, the Lorentz gas was introduced as a model of electronic gas in metals which occurred to be completely irrelevant. Likewise, the Ehrenfests' Wind-Tree model is considered to be irrelevant as a model for diffusion and moved from statistical mechanics to pure mathematics where it is very popular now [39, 40, 44, 45, 46, 47, 48, 49, 50].

Our goal in this chapter is to demonstrate that in fact, the Wind-Tree model is a good model to study diffusion and its dynamics is even richer than every bodies favorite Lorentz

gas. Although we study only the physical periodic Wind-Tree model, it is quite clear that the non-periodic Wind-Tree model is probably dynamically richer than the (physical and mathematical) Lorentz gas with the same configuration in the plane of the centers of scatterers, but at least it has all the regimes of diffusion which the non-periodic Lorentz gas does.

A key observation is that a physical Wind-Tree model becomes a semi-dispersing billiard for any positive radius $r$ of a hard ball (disk in $\mathbf{R}^2$), whereas a physical Sinai billiard always remains Sinai billiard for any $r > 0$. Therefore, in case of a bounded free path (finite horizon) both periodic Lorentz gas and periodic Wind-Tree model demonstrate diffusive behavior. However, if a free path is unbounded then dynamics of both periodic systems becomes superdiffusive and it is where Wind-Tree model overpasses Lorentz gas. If the configuration of scatterers is periodic then the particle may have unbounded free path only in strips on plane bounded by two parallel lines. Such strips traditionally are called corridors. In periodic Lorentz gas with unbounded free path, there is only one type of corridors, while in the periodic Wind-Tree model there are two types of corridors. Presence of a corridor of the first type results in the $(\ln t)$ growth of the diffusion coefficient while corridors of the second type make it grow as $(\ln t)^2$.

The structure of this chapter is the following. In Section 2 we introduce the necessary notations and study some properties of the Ehrenfests' Wind-Tree model with infinite horizon. Section 3 and 4 deal with the calculation of the tail of the distribution of the free motion vectors (displacement) in two different types of corridors. In Section 5 an estimation of their correlations is given and the limit distributions of properly normalized free motion vectors in both discrete and continuous-time dynamics are discussed.

## 4.1 Ehrenfests' Wind-Tree Model

### 4.1.1 Configuration Space

The basic scatterers $S$ in Ehrenfests' Wind-Tree model are rhombuses. Each scatterer is determined by two parameters $\theta$ and $a$, where $2\theta$ is the acute angle of this scatterer and $a$ is its side length. Moreover, we assume that the diagonals of scatterers are parallel to $x$ and $y$-axes in $\mathbf{R}^2$ and acute angles are top and bottom angles of them. Then, in the periodic Ehrenfests' Wind-Tree model there is a periodic configuration of these basic scatterers with centers at the points with integer coordinates in $\mathbf{R}^2$ (Fig. 4.1a). Thus, a periodic Wind-Tree model is an unfolding of a billiard in a torus $\mathbf{T}^2$ with the scatterer $S$ where both are centered at the origin (Fig. 4.1b).

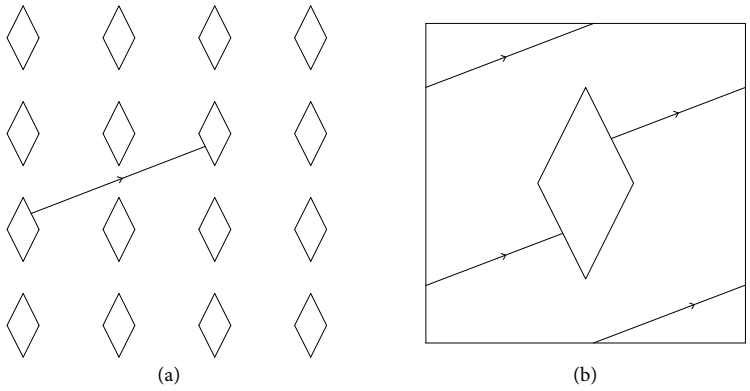


Figure 4.1: (a) Periodic Ehrenfests' Wind-Tree model. (b) Ehrenfests' Wind-Tree model in torus.

A configuration of scatterers is said to have a finite horizon if there exists $L > 0$ such that any straight segment of the length bigger than $L$ in $\mathbf{R}^2$ intersects at least one scatterer (see Fig. 4.2b where we have two types of rhombuses). This means that the length of the free motion of the particle is bounded. Otherwise, the configuration of scatterers has an infinite horizon. When we have a configuration of scatterers with an infinite horizon, an open strip of parallel straight lines which intersects no scatterers is called a corridor. Moreover, a corridor has two opposite directions defined by the directions of parallel lines that bound

the corridor. We will call two corridors equivalent if they have the same directions.

### 4.1.2 Corridors in Ehrenfests' Wind-Tree Model

The width of a corridor is defined by the distance between its boundary lines. The periodic Ehrenfests' Wind-Tree model, described in section 4.1.1, can have two types of corridors:

- Type I: Corridors with boundaries touching some vertices of scatterers.
- Type II: Corridors with boundaries containing some edges of scatterers.

When $2a\cos\theta < 1$, there exist horizontal and vertical corridors denoted by $C_h$ and $C_v$, respectively, and we call them corridors of type I (Fig. 4.2a). Their widths $d_h$ and $d_v$ are equal to:

$$d_h = 1 - 2a\cos\theta, \qquad d_v = 1 - 2a\sin\theta,$$

respectively. In addition, for some choices of parameters $a$ and $\theta$ there exist oblique corridors which could be either of type I or II. We will denote the oblique corridors by $C_o$ and their width by $d_o$. (Fig. 4.2a)

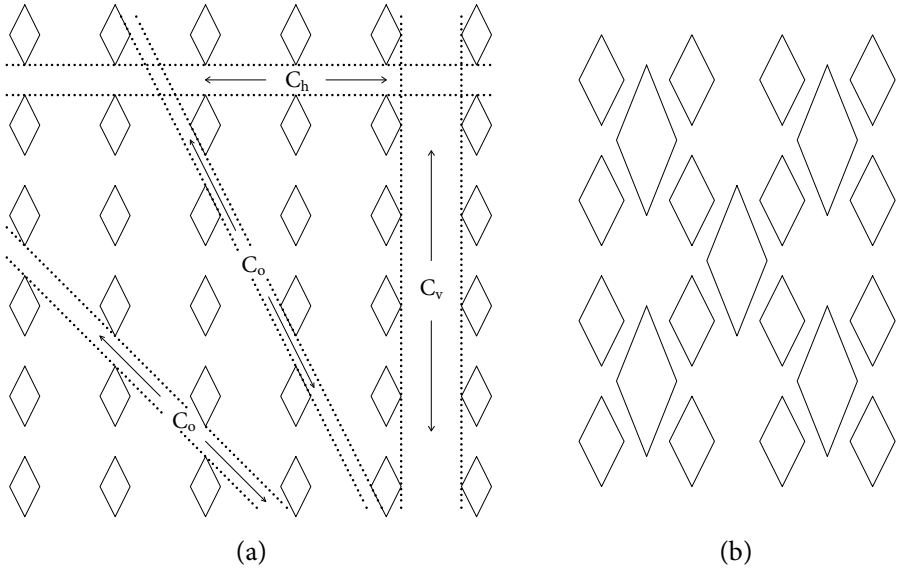


Figure 4.2: (a) Periodic Ehrenfests' Wind-Tree model with corridors: $C_h$, $C_v$, and $C_o$. (b) A periodic Ehrenfests' Wind-Tree model with a finite horizon and two types of rhombuses.

**Lemma 4.1.1.** *There is an oblique corridor of type II if and only if* $\tan\theta = \frac{m}{n}$ *and*

$$a < \frac{\cos\theta + \sin\theta - \lceil \frac{n}{m} \rceil \sin\theta}{\sin(2\theta)} = \frac{(m+n-\lceil \frac{n}{m} \rceil m)\sqrt{m^2+n^2}}{2mn}, \tag{4.1}$$

*where* $0 < m \leq n$ *are integers. Moreover,*

$$d_o = \sin\theta + \cos\theta - \lceil \frac{n}{m} \rceil \sin\theta - a\sin(2\theta) = \frac{m+n-\lceil \frac{n}{m} \rceil m}{\sqrt{m^2+n^2}} - \frac{2mna}{m^2+n^2}.$$

*Proof.* From the definition of corridors of type II and $\theta$, it is obvious that $\tan\theta \leq 1$ is a rational number. To calculate the width of these corridors, we need to consider a passage by the particle through a corridor between two adjunct columns of rhombuses. According to Figure 4.3,

$$|CF| = 1, \quad |EF| = a\sin\theta, \quad \tan\theta = \frac{|CD|}{|AB|+|BC|} = \frac{|CD|}{a\cos\theta + (\lceil \frac{n}{m} \rceil - 1)}.$$

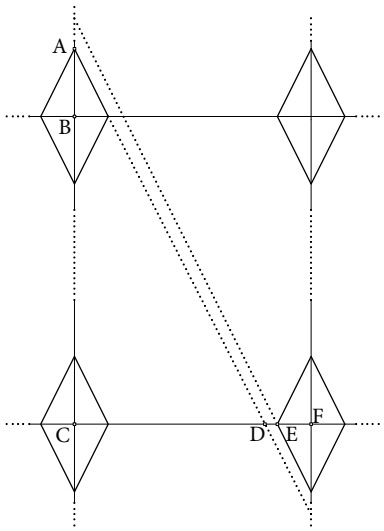


Figure 4.3: A passage through a corridor of type II between two adjunct columns of rhombuses.

Therefore,

$$|DE| = 1 - |EF| - |CD| = 1 - a\sin\theta - \Big(\lceil\frac{n}{m}\rceil - 1 + a\cos\theta\Big)\tan\theta.$$

Finally,

$$\begin{aligned} d_o = |DE|\cos\theta &= \sin\theta + \cos\theta - \lceil\frac{n}{m}\rceil\sin\theta - a\sin(2\theta) \\ &= \frac{m+n-\lceil\frac{n}{m}\rceil m}{\sqrt{m^2+n^2}} - \frac{2mna}{m^2+n^2}. \end{aligned}$$

Solving the inequality $d_o > 0$ for parameter $a$, we obtain:

$$a < \frac{\cos\theta + \sin\theta - \lceil\frac{n}{m}\rceil\sin\theta}{\sin(2\theta)} = \frac{(m+n-\lceil\frac{n}{m}\rceil m)\sqrt{m^2+n^2}}{2mn}.$$

These calculations also show that if $\tan\theta = \frac{m}{n}$ and the inequality (4.1) are satisfied then $d_o > 0$, where $d_o$ is the width of the oblique corridor of type II. □

Let $\alpha$ be the angle between the axis of an oblique corridor of type I and the positive $y$-axis such that $-\frac{\pi}{2} < \alpha < \frac{\pi}{2}$. It is easy to see that $\alpha \notin \{0, \pm\theta\}$.

**Lemma 4.1.2.** *The following relations hold for an oblique corridor of type I.*

1. $|\tan(\alpha)| = \frac{m}{n}$ *for some integers* $n > 0$ *and* $m > 0$.

2. *If* $|\tan(\alpha)| < \tan\theta$, *then*

   $$d_o = \cos\alpha + \sin\alpha - \lceil\frac{n}{m}\rceil\sin\alpha - 2a\sin\theta\cos\alpha = \frac{\big(n+m-m\lceil\frac{n}{m}\rceil - 2an\sin\theta\big)}{\sqrt{n^2+m^2}},$$

   *where* $a < \frac{n+m-m\lceil\frac{n}{m}\rceil}{2n\sin\theta}$.

3. *If* $\tan\theta < |\tan(\alpha)| \leq 1$, *then*

   $$d_o = \cos\alpha + \sin\alpha - \lceil\frac{n}{m}\rceil\sin\alpha - 2a\sin\alpha\cos\theta = \frac{\big(n+m-m\lceil\frac{n}{m}\rceil - 2am\cos\theta\big)}{\sqrt{n^2+m^2}},$$

*where* $a < \frac{n+m-m\lceil \frac{n}{m} \rceil}{2m\cos\theta}$.

4. *If* $1 < |\tan(\alpha)|$, *then*

$$d_o = \cos\alpha + \sin\alpha - \lceil \frac{m}{n} \rceil \cos\alpha - 2a\cos\theta\sin\alpha = \frac{\left(n+m-n\lceil \frac{m}{n} \rceil - 2am\cos\theta\right)}{\sqrt{n^2+m^2}},$$

*where* $a < \frac{n+m-n\lceil \frac{m}{n} \rceil}{2m\cos\theta}$.

*Proof.* The proof is omitted since it is very similar to the proof of Lemma 4.1.1. □

### 4.1.3 Physical Ehrenfests' Wind-Tree Model

Physical billiards (i.e. billiards with a moving hard ball like a ball in real billiard as well as in all real systems modeled by billiards) were introduced and studied in [10]. A ball there and in this chapter is assumed to be a smooth hard ball. In case of a rough ball, it acquires rotation after collision at any point of the boundary [51].

It is easy to see that dynamics of a physical Lorentz gas is the same for any radius $r$ of the moving physical particle (of course unless $r$ becomes so big that the particle gets stuck in some subset of the plane). Indeed the scatterers remain to be circles but their radius increases by $r$. A totally different situation occurs in the Wind-Tree model where boundaries of scatterers acquire dispersing components (arcs of a circle of radius $r$).

In what follows, we will consider the mathematical billiard equivalent to the motion of a physical particle (disk) of radius $r > 0$ in the periodic Ehrenfests' Wind-Tree model. We will use notations $S'$ and $\partial S'$ for the scatterer and its boundary in the equivalent mathematical billiard, respectively. (See Fig. 4.4)

There are still two types of corridors in the equivalent mathematical billiard of the physical periodic Wind-Tree model:

- Type I: Corridors with boundaries tangent to the dispersing components of scatterers.

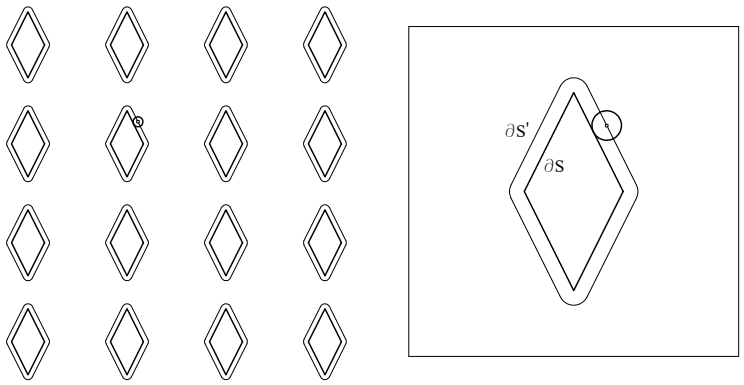


Figure 4.4: Physical Ehrenfests' Wind-Tree model and its equivalent mathematical billiard.

- Type II: Corridors with boundaries containing the flat (neutral) components of scatterers.

Corridors remain if $r$ is small enough. More precisely, if $C$ is a corridor of type I (or II) in a physical periodic Ehrenfests' Wind-Tree model with the width $d$ and the physical particle has radius $r > 0$ such that $d > 2r$, then the equivalent mathematical billiard will have a corridor of type I (or II) in the same directions of $C$ with the width $d - 2r$.

In the sequel, we will use the same notations $d_h$, $d_v$, and $d_o$ to denote the width of horizontal, vertical, and oblique corridors, respectively, in the equivalent mathematical billiard.

### 4.1.4 Dynamics of the Physical Ehrenfests' Wind-Tree model

In this section, we introduce phase space of the system in the folded configuration space in torus.

Denote by $x(t)$ the position of the center of the physical particle at time $t$. We will characterize reflections by two quantities: $s$ the coordinate of the reflection point on $\partial S'$ with respect to the natural arc length $|.|$ in $\mathbf{R}^2$, and $\varphi$ the angle of reflection (the angle with the sign between the velocity vector after the reflection and the outer normal vector at the reflection point). Therefore, the phase space is:

$$\Lambda = \{X = (s, \varphi) \mid 0 \leq s < |\partial S'|, \ -\frac{\pi}{2} \leq \varphi \leq \frac{\pi}{2}\}.$$

Now, let $T : \Lambda \to \Lambda$ be the Poincare section billiard map of the system such that $T(X_n) = T(s_n, \varphi_n) = (s_{n+1}, \varphi_{n+1}) = X_{n+1}$. This map preserves the Liouville measure:

$$\mu(d\varphi ds) = Z^{-1} \cos(\varphi) d\varphi ds, \tag{4.2}$$

where,

$$Z = \int_{\partial S'} \int_{-\pi/2}^{\pi/2} \cos(\varphi) d\varphi ds = 2|\partial S'|,$$

on $\Lambda$. Moreover, the expected value of the function $F(X)$ is defined by:

$$\langle F(X) \rangle := \int_{\Lambda} F(X) \mu(d\varphi ds) = Z^{-1} \int_{\partial S'} \int_{-\pi/2}^{\pi/2} F(X) \cos(\varphi) d\varphi ds,$$

where $X = (s, \varphi)$.

Let $x_n = x(X_n) \in \mathbf{R}^2$ be the position of the center of the physical particle in the discrete system at $n^{th}$ reflection. We will denote the segment (link) of the trajectory after $n^{th}$ reflection by $[x_n, x_{n+1}]$ and the corresponding vector of this free motion (displacement) by:

$$r(X_n) := x(TX_n) - x(X_n) = x(X_{n+1}) - x(X_n) = x_{n+1} - x_n.$$

This implies,

$$x_n - x_0 = x(T^n X_0) - x(X_0) = \sum_{i=0}^{n-1} r(T^i X_0). \tag{4.3}$$

According to (4.3), the problem of studying the statistical properties of the vector $x_n - x_0 = x(T^n X_0) - x(X_0)$, when $n \to \infty$, is reduced to the problem about statistical properties of the free motion vector $r(X)$ with respect to the billiard map $T$. Let $\nu$ be the probability distribution of the free motion vector $r(X)$ with respect to Liouville measure $\mu$.

**Corollary 4.1.3.** *The distribution $\nu$ is symmetric.*

*Proof.* It is analogous to the proof of Proposition 4.1 of [41]. □

In the following sections, we will study some properties of the distribution $\nu$ and of the

second moment $\langle (r(X), r(T^n X)) \rangle$, where $(.,.)$ denotes the standard inner product in $\mathbf{R}^2$ .

## 4.2 Asymptotics of $\nu$ in Corridors of Type I

From Section 4.1.3, we know that the boundary of a corridor of type I is tangent to the dispersing components of $\partial S'$. In the following lemma we will show that for a long enough segment $[x_0, x_1]$ in a corridor of type I, the endpoints $x_0$ and $x_1$ are on those dispersing parts of $\partial S'$ which are tangent to the boundary of the corridor.

**Lemma 4.2.1.** *Consider a finite segment $[x_0, x_1]$ of length $|r(X_0)| = |x_1 - x_0| = L$ in a corridor of type I with the width $d$. There exists a constant $L_0 > 0$ such that if $L > L_0$, then the points $x_0$ and $x_1$ are on dispersing parts of $\partial S'$ which are tangent to the boundary of that corridor on its opposite sides.*

*Proof.* Let $\alpha$ be the angle between the direction of the corridor of type I and the positive $y$-axis as it is shown in Fig. 4.5. First, we prove this lemma when $\alpha > \theta$. According to the Fig. 4.5,

$$|DC| = |DB| = r, \qquad \beta := \angle CDB = \alpha - \theta, \qquad |AB| = \frac{1}{\sin \alpha}.$$

Moreover, the distance between the point $C$ and the boundary of the corridor is equal to $r - r\cos\beta$. This implies that,

$$\sin(\angle CAB) > (r - r\cos\beta)\sin\alpha = (r - r\cos(\alpha - \theta))\sin\alpha.$$

If we denote by $L$ the length of the longest segment in this corridor with one endpoints at $C$, then:

$$L < \frac{d}{\sin(\angle CAB)} + 2|AB| < \frac{d}{(r - r\cos(\alpha - \theta))\sin\alpha} + \frac{2}{\sin\alpha}.$$

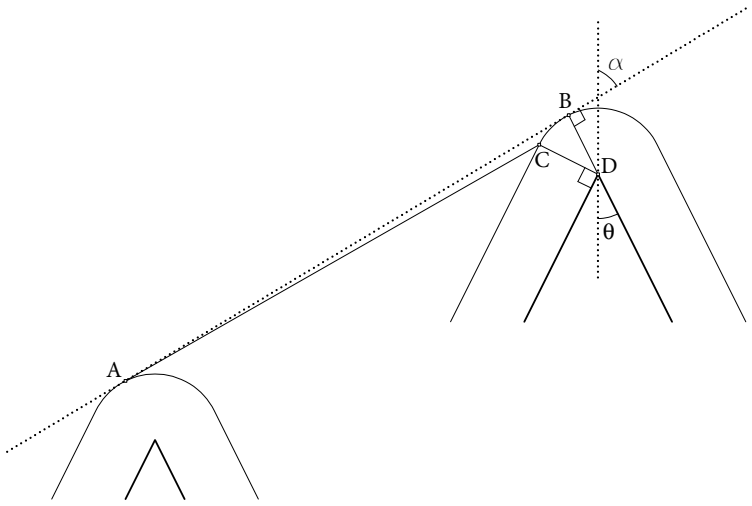


Figure 4.5: A Segment with an endpoint on a dispersing part tangent to a corridor of type I.

To complete the proof for this case, let $L_0 = \frac{d}{(r - r\cos(\alpha-\theta))\sin\alpha} + \frac{2}{\sin\alpha}$.

In case $\alpha < \theta$, the corridor is tangent to the dispersing components on left and right sides of $\partial S'$. The proof in this case is very similar to the previous one, and it results at:

$$L_0 = \frac{d}{(r - r\cos(\theta - \alpha))\cos\alpha} + \frac{2}{\cos\alpha},$$

when $\alpha < \theta$. □

Let $L_h$ and $L_v$ denote the parameter $L_0$ from Lemma 4.2.1, respectively, for the horizontal and vertical corridors $C_h$ and $C_v$. Then,

$$L_h = \frac{d_h}{r - r\sin\theta} + 2, \qquad L_v = \frac{d_v}{r - r\cos\theta} + 2.$$

Consider the segment $[x_0, x_1]$ is in $C_h$ or $C_v$ such that $|x_0 - x_1| > \max\{L_h, L_v\}$. If $y_0$ and $y_1$ are the intersection points of this segment with the boundary of the corridor (Fig. 4.4), then

$$|x_0 - y_0| < 1, \qquad |x_1 - y_1| < 1. \tag{4.4}$$

From Lemma 4.2.1, we know that $x_0$ and $x_1$ are on dispersing components of $\partial S'$. Let

$A$ and $B$ denote the tangent points to the boundaries of the corridor of those dispersing components which contain the points $x_0$ and $x_1$, respectively. (Fig. 4.6)

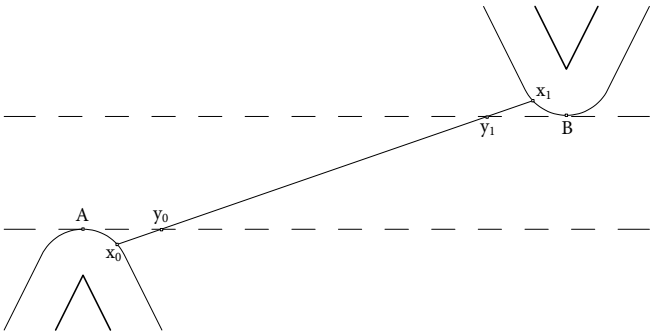


Figure 4.6: Intersection of a finite segment $[x_0, x_1]$ with the boundary of $C_h$.

**Lemma 4.2.2.** *If $[x_0, x_1]$ is a segment in $C_h$ or $C_v$ such that $|x_0 - x_1| > \max\{L_h, L_v\}$, then there exists an $\epsilon > 0$ such that:*

$$|x_0 - A| < \epsilon, \qquad\qquad |x_1 - B| < \epsilon.$$

*Moreover, $|x_0 - A|$ and $|x_1 - B|$ tend to zero when $|x_0 - x_1| \to \infty$.*

*Proof.* It is easy to see that $\epsilon = r(\frac{\pi}{2} - \theta)$. Moreover, the calculation in the proof of Lemma 4.2.1 suggests that $|x_0 - A|$ and $|x_1 - B|$ tend to zero when $|x_0 - x_1| \to \infty$. □

The inequalities in (4.4) and lemmas 4.2.1 and 4.2.2 guarantee that asymptotics of the probability of free motion vectors in horizontal and vertical corridors of the periodic Ehrenfests' Wind-Tree model is the same as asymptotics of the probability of free motion vectors in corridors of the periodic Lorentz gas [41]. According to the result of proposition 4.2 in [41], the expressions for the corresponding probabilities in the limit $L \to \infty$ are:

$$\begin{aligned} \mathbf{Pr}_h(L) :=& Probability\ of\ \{r(X)\ in\ C_h\ such\ that\ |r(X)| > L\} \\ =& \frac{Z^{-1} d_h^2}{L^2} + O(L^{-5/2}), \end{aligned} \tag{4.5}$$

and

$$\begin{aligned}\mathbf{Pr}_v(L) :=& Probability\ of\ \{r(X)\ in\ C_v\ such\ that\ |r(X)| > L\} \\ =& \frac{Z^{-1}d_v^2}{L^2} + O(L^{-5/2}).\end{aligned} \tag{4.6}$$

### 4.3 Asymptotics of $\nu$ in Corridors of Type II

Our main result is concerned with oblique corridors of type II, where the boundary of the corridor contains flat components of scatterers. We will show that the existence of such corridors results in stronger superdiffusive regimes than the one in the Lorentz gas.

From Lemma 4.2.1, we can expect oblique corridors of type I to have the same diffusive properties as the horizontal and vertical corridors. To reduce the volume of calculations, we will consider a physical periodic Ehrenfests' Wind-Tree model without oblique corridors of type I. Moreover, if there exists an oblique corridor of type II where $\theta \neq \frac{\pi}{4}$, then the scatterers are distributed over the boundary of this corridor in a way that any trajectory in this corridor is likely to leave the corridor after a few reflections on neutral parts of scatterers (See Fig. 4.7).

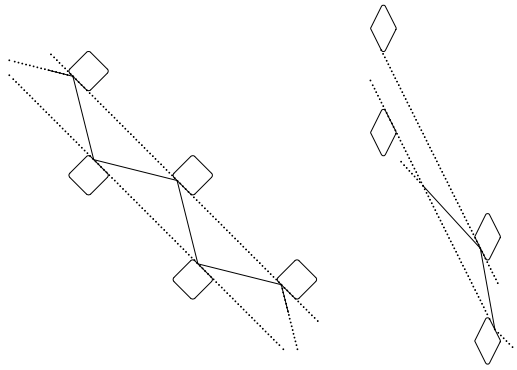

Figure 4.7: Trajectories with reflections on neutral parts in a corridor of type II when $\theta = \pi/4$ (left) and $\theta \neq \pi/4$ (right).

By Lemma 4.1.2, one can calculate the minimum value of $a$ such that there is no oblique corridor of type I when $\theta = \frac{\pi}{4}$. Since $\tan(\theta) = 1$, we only need to consider cases 2 and 4 in

Lemma 4.1.2. Moreover, under this assumption, the upper bounds of $a$ in these two cases will be the same and equal to:

$$\frac{n+m-m\lceil\frac{n}{m}\rceil}{\sqrt{2}n},$$

where $0<m<n$ are integers. Therefore, if $\theta=\frac{\pi}{4}$ and

$$a \geq Max_{\{(n,m)|\ n>m,\ n,m\in\mathbf{N}\}}\left\{\frac{n+m-m\lceil\frac{n}{m}\rceil}{\sqrt{2}n}\right\}=\frac{\sqrt{2}}{4},$$

then there are no oblique corridors of type I.

In the rest of this chapter, we consider physical periodic Ehrenfests' Wind-Tree model with a moving disk of radius $0<r<\frac{\sqrt{2}}{8}$ where $\theta=\frac{\pi}{4}$ and $\frac{\sqrt{2}}{4}\leq a<\frac{\sqrt{2}}{2}-2r$.

Thus, our model has two corridors of type I ($C_h$ and $C_v$) and two corridors of type II with directions parallel to $y=x$ and $y=-x$. Denote these oblique corridors of type II by $C_o^+$ and $C_o^-$, respectively.

To estimate the tail of the distribution $\nu$ in this model along corridors $C_o^+$ and $C_o^-$, we need to calculate the asymptotics of

$$\begin{aligned}\mathbf{Pr}_o(L) :=& Probability\ of\ \{r(X)\ in\ C_o^+\ such\ that\ |r(X)|>L\}\\ =& Probability\ of\ \{r(X)\ in\ C_o^-\ such\ that\ |r(X)|>L\}\end{aligned}$$

when $L\to\infty$.

**Proposition 4.3.1.** *When $L\to\infty$,*

$$\mathbf{Pr}_o(L)=aZ^{-1}\left(\frac{d_o}{L}\right)^2+O(L^{-3}), \tag{4.7}$$

*where $d_o$ is the width of oblique corridors $C_o^+$ or $C_o^-$.*

*Proof.* According to the Fig. 4.8, in the oblique corridors of type II of the physical periodic

Wind-tree model:

$$w := \tan(\varphi) = \frac{z-t}{d_o} \implies \cos(\varphi)d\varphi = \frac{dz}{d_o(1+w^2)^{3/2}}.$$

Therefore, the probability density function $f(.)$ of the distribution of $z$ with respect to the

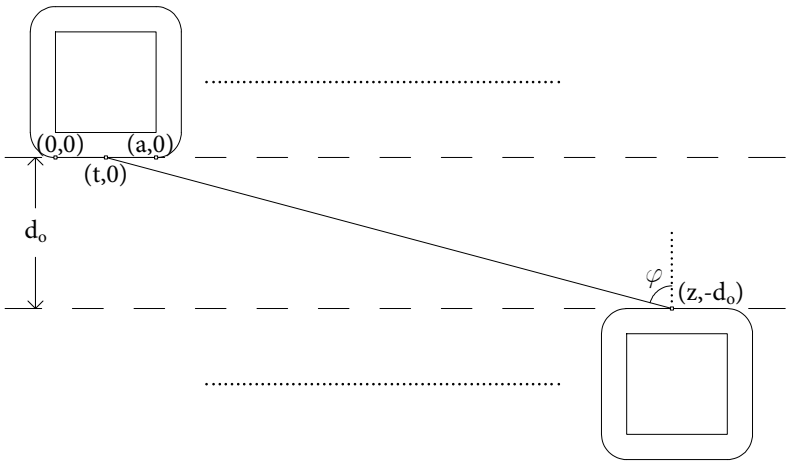


Figure 4.8: A long collision free segment in an oblique corridor of type II.

Liouville measure $Z^{-1}\cos(\varphi)d\varphi ds$ along these corridors is equal to:

$$f(z) = \int_0^a \frac{Z^{-1}}{d_o(1+w^2)^{3/2}}dt = Z^{-1}d_o^2\int_0^a \frac{dt}{(d_o^2+(z-t)^2)^{3/2}}$$

$$\simeq Z^{-1}d_o^2\int_0^a \frac{dt}{(z-t)^3} = \frac{Z^{-1}d_o^2}{2}\left(\frac{1}{(z-a)^2}-\frac{1}{z^2}\right) = \frac{aZ^{-1}d_o^2}{z^3}(1+O(z^{-1})).$$

Hence, the probability of $|r(X_0)| > L$ is given by:

$$\begin{aligned}\mathbf{Pr}_o(L) =& 2\int_L^\infty f(z)dz = 2\int_L^\infty \frac{aZ^{-1}d_o^2}{z^3}(1+O(z^{-1}))dz \\ =& aZ^{-1}\left(\frac{d_o}{L}\right)^2 + O(L^{-3}).\end{aligned} \tag{4.8}$$

□

The factor 2 in the expression for $\mathbf{Pr}_o(L)$ in the equation (4.8) appears because there are two opposite directions in each corridor.

**Proposition 4.3.2.** $\langle r(X)\rangle = 0$, $\langle |r(X)|\rangle < \infty$, *and* $\langle |r(X)|^2\rangle = \infty$. *Moreover, if* $\phi_R(x) = |x|^2$ *when* $|x| < R$ *and it is zero otherwise, then*

$$\langle \phi_R(r(X))\rangle = Const.\ln(R) + O(1),$$

*when* $R \to \infty$.

*Proof.* We have:

$$\langle r(X)\rangle = \int r(X)\mu(d\varphi ds) = 0,$$

because $\nu$ is symmetric (Proposition 4.1.3). If $L$ is sufficiently large, then it follows from (4.5-4.7) that:

$$\begin{aligned}
\langle |r(X)|\rangle &= \int |r(X)|\mu(d\varphi ds) = \int_{|r|\le L} |r(X)|\mu(d\varphi ds) + \int_{|r|>L} |r(X)|\mu(d\varphi ds) \\
&= \int_{|r|\le L} |r(X)|\mu(d\varphi ds) + \int_{\substack{|r|>L \\ in\ C_o^+}} |r(X)|\mu(d\varphi ds) + \int_{\substack{|r|>L \\ in\ C_o^-}} |r(X)|\mu(d\varphi ds) \\
&\qquad + \int_{\substack{|r|>L \\ in\ C_h}} |r(X)|\mu(d\varphi ds) + \int_{\substack{|r|>L \\ in\ C_v}} |r(X)|\mu(d\varphi ds) \\
&< L + 2\int_L^\infty \frac{2aZ^{-1}d_o^2}{x^2}dx + \int_L^\infty \frac{2Z^{-1}d_h^2}{x^2}dx + \int_L^\infty \frac{2Z^{-1}d_v^2}{x^2}dx < \infty.
\end{aligned}$$

Finally, for $R \to \infty$:

$$\begin{aligned}
\langle \phi_R(r(X))\rangle =& \int_{|r|\le L<R} |r(X)|^2\mu(d\varphi ds) + \int_{L<|r|<R} |r(X)|^2\mu(d\varphi ds) \\
=& M_0 + \int_{\substack{L<|r|<R \\ in\ C_o^+}} |r(X)|^2\mu(d\varphi ds) + \int_{\substack{L<|r|<R \\ in\ C_o^-}} |r(X)|^2\mu(d\varphi ds) \\
&+ \int_{\substack{L<|r|<R \\ in\ C_h}} |r(X)|^2\mu(d\varphi ds) + \int_{\substack{L<|r|<R \\ in\ C_v}} |r(X)|^2\mu(d\varphi ds) \\
=& M_0 + 2\int_L^R \frac{2aZ^{-1}d_o^2}{x}dx + \int_L^R \frac{2Z^{-1}d_h^2}{x}dx + \int_L^R \frac{2Z^{-1}d_v^2}{x}dx \\
=& Const.\ln(R) + O(1).
\end{aligned}$$

Therefore, $\langle |r(X)|^2 \rangle = \infty$. $\square$

## 4.4 Statistical Properties of Ehrenfests' Wind-Tree Models

In the previous section, we studied the asymptotic behavior of the distribution $\nu$ of the free motion vector $r(X) = x(TX) - x(X)$. Now, we will consider the joint distribution $\nu_n$ of vectors $r(X)$ and $r(T^n X)$ with respect to the Liouville measure $\mu$ in order to estimate,

$$\langle |r(X)||r(T^n X)| \rangle,$$

for any $n \neq 0$.

**Proposition 4.4.1.** *The distribution $\nu_n$ is invariant with respect to the transformation $(r_1, r_2) \mapsto -(r_2, r_1)$.*

The proof is identical to the proof of Proposition 5.1 in [41]. Moreover, the Proposition 4.4.1 implies,

$$(|r(X_0)|, |r(T^n X_0)|) \stackrel{d}{=} (|r(T^n X_0)|, |r(X_0)|).$$

### 4.4.1 Estimation of Correlations of Free Motion Vectors

Let $r(X_0) = [x_0, x_1]$ be in $C_o^+$ or $C_o^-$ and $x_1$ be on a neutral component of $\partial S'$ belongs to the boundary of that corridor. Then quantities $|r(X_0)|$ and $|r(TX_0)|$ satisfy the relation:

$$|r(TX_0)| = |r(X_0)| + O(1). \tag{4.9}$$

More generally, when endpoints of segments $r(T^{i-1}X_0) = r(X_{i-1}) = [x_{i-1}, x_i]$ for $i = 1, \ldots, n$ belong to neutral components of $\partial S'$ which are in the boundary of a corridor of type II, then:

$$|r(X_i)| = |r(T^i X_0)| = |r(X_0)|, \tag{4.10}$$

for $i = 1, 2, \ldots, n-1$, and

$$|r(X_0)| \leq |r(X_n)| = |r(T^n X_0)| < |r(X_0)| + 1. \tag{4.11}$$

Denote the expected value of a function along the corridors $C_o^+$ or $C_o^-$ by $\langle . \rangle_o$.

**Proposition 4.4.2.** *Let all $x_i$ of segments $r(T^i X) = [x_i, x_{i+1}]$ for $i = 0, 1, \ldots, n$ belong to neutral components of $\partial S'$ in the boundary of $C_o^+$ or $C_o^-$, then*

$$\langle |r(X)||r(T^{n-1}X)| \rangle_o = \frac{\langle |r(X)|^2 \rangle_o}{n}.$$

*Proof.* First, we find the probability of trajectories with $n$ consecutive reflections on neutral parts of $\partial S'$ in the boundary of a corridor of type II.

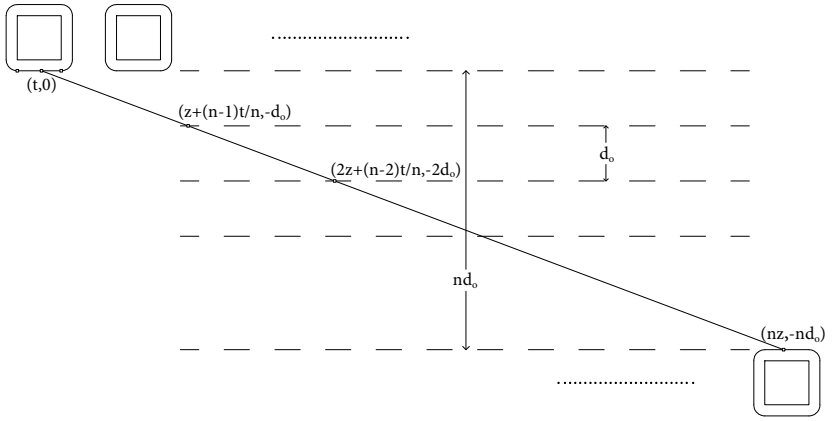


Figure 4.9: Segments with reflections on neutral components of $\partial S'$ in boundaries of a corridor of type II.

It follows from Fig. 4.9 that,

$$w = \tan(\varphi) = \frac{nz - t}{nd_o} \implies \cos(\varphi) d\varphi = \frac{dz}{nd_o(1 + w^2)^{3/2}}.$$

Then,

$$\begin{aligned} f_n(z) :=& \int_0^a \frac{Z^{-1}}{nd_o(1+w^2)^{3/2}}dt = Z^{-1}n^2d_o^2\int_0^a \frac{dt}{(n^2d_o^2+(nz-t)^2)^{3/2}} \\ \simeq& Z^{-1}n^2d_o^2\int_0^a \frac{dt}{(nz-t)^3} = \frac{Z^{-1}n^2d_o^2}{2}\left(\frac{1}{(nz-a)^2}-\frac{1}{n^2z^2}\right) \\ =& \frac{aZ^{-1}d_o^2}{nz^3}(1+O(z^{-1})). \end{aligned} \tag{4.12}$$

The equation (4.12) and Proposition 4.3.1 show that,

$$f_n(z) = \frac{1}{n}f(z). \tag{4.13}$$

Let $P_n(L)$ denote the probability of orbits with segments $[x_i, x_{i+1}]$ for $i = 0, 1, \ldots, n$ such that all $x_i$ are on the neutral parts in the boundary of a corridor of type II and $|x_{i+1}-x_i| > L$. Then, it follows from (4.13) and the proof of Proposition 4.3.1 that,

$$P_n(L) = \frac{1}{n}\mathbf{Pr}_o(L).$$

Moreover, the equation (4.10) implies,

$$|r(X)||r(T^{n-1}X)| = |r(X)|^2.$$

Therefore,

$$\langle |r(X)||r(T^{n-1}X)|\rangle_o = \frac{\langle |r(X)|^2\rangle_o}{n}.$$

□

We will now estimate $\langle |r(X)||r(T^{n-1}X)|\rangle_o$ where some $x_i$ for $i = 0, 1, 2, \ldots, n$ belongs to the dispersing parts of $\partial S'$. Let consider the case that there is a reflection off a dispersing component and it is followed by $n$ consecutive reflections on neutral parts in the boundary of a corridor of type II. The proof of Proposition 4.4.2, particularly the equation

(4.12), shows that:

$$\langle |r(X)||r(T^n X)| \rangle_o = \frac{\langle |r(X)||r(TX)| \rangle_o}{n},$$

where $x_1$ in $r(X) = [x_0, x_1]$ is on a dispersing component. Then, proposition 5.3 in [41] implies that $\langle |r(X)||r(TX)| \rangle_o = Const.$ Therefore, in this case

$$\langle |r(X)||r(T^n X)| \rangle_o = \frac{\langle |r(X)||r(TX)| \rangle_o}{n} = \frac{O(1)}{n}. \tag{4.14}$$

More generally, when an orbit has only reflections on neutral parts in the boundary of a corridor of type II, the angle between its segments and the length of its segments remain the same, while reflections on dispersing components change these angles and they also change lengths of free paths. The average of these changes (correlations) is estimated in theorem 5.6 in [41] when an orbit has only reflections on dispersing components. The results of [41] and Proposition 4.4.2 show that when an orbit has more than one reflection on dispersing components, the correlations is smaller than the correlations in the case where there is only one reflection on a dispersing part when the particle goes along a corridor of type II. Hence, from the equation (4.14) and Proposition 4.4.2, the correlation function in a corridor of type II satisfies the following relation:

$$\langle (r(X), r(T^n X)) \rangle_o \simeq \langle |r(X)||r(T^n X)| \rangle_o = \frac{\langle |r(X)|^2 \rangle_o + O(1)}{n+1}, \tag{4.15}$$

since $r(X)$ and $r(T^n X)$ have almost the same directions in that corridor of type II (i.e. $(r(X), r(T^n X)) \simeq |r(X)||r(T^n X)|$).

To better understand this result observe that two neighboring boundary components of a straight segment in the boundary of any scatterer are arcs of a circle with the same radius. Therefore their combined influence on correlations is the same as in the Lorentz gas [41]. Indeed, by putting them together we get circular part of scatterer which influences the passage of a particle through the corridor. The fact that dispersing components are apart

on the length of a neutral component clearly contributes only to a constant factor in the estimate of correlations.

### 4.4.2 Statistical Behavior of Trajectories in Discrete Dynamics

From the result of previous sections, one can expect that the physical periodic Ehrenfests' Wind-Tree models will have more regimes of diffusion than the Lorentz gas. To show that we need to estimate $\langle |x(T^n X) - x(X)|^2 \rangle$ when $n \to \infty$. This value can be written as:

$$\begin{aligned} \langle |x(T^n X) - x(X)|^2 \rangle &= \sum_{i=0}^{n-1} \sum_{j=0}^{n-1} \langle (r(T^i X), r(T^j X)) \rangle \\ &= n \langle |r(X)|^2 \rangle + 2 \sum_{j=1}^{n-1} (n-j) \langle (r(X), r(T^j X)) \rangle. \end{aligned} \tag{4.16}$$

It follows from (4.15) that,

$$\begin{aligned} \lim_{n\to\infty} \sum_{k=1}^{n} \langle (r(X), r(T^k X)) \rangle_o &\simeq \lim_{n\to\infty} \sum_{k=1}^{n} \frac{\langle |r(X)|^2 \rangle_o + O(1)}{k+1} \\ &= \lim_{n\to\infty} [(\ln(n) - 1) \langle |r(X)|^2 \rangle_o + O(\ln n)]. \end{aligned} \tag{4.17}$$

Moreover, Proposition 4.3.2 implies:

$$\begin{aligned} \langle \phi_R(r(X)) \rangle_o &= \int_{\substack{|r| \le L < R \\ in\ C_o^+}} |r(X)|^2 \mu(d\varphi ds) + \int_{\substack{L < |r| < R \\ in\ C_o^+}} |r(X)|^2 \mu(d\varphi ds) \\ &= m_0 + 2 \int_L^R \frac{a Z^{-1} d_o^2}{x} dx = \frac{2 a d_o^2}{Z} \ln R + O(1), \end{aligned} \tag{4.18}$$

when $R \to \infty$. It follows from equations (4.17) and (4.18) that,

$$\sum_{k=1}^{N} \langle (r(X), r(T^k X)) \rangle_o = \frac{2 a d_o^2}{Z} (\ln N)^2 + O(\ln N). \tag{4.19}$$

Therefore the main contribution to correlations is made by orbits propagating in corridors of type II and reflecting only off neutral components of the boundary.

Consider a physical periodic Wind-Tree model. Then for any positive radius $r > 0$ of the moving particle we conjecture that the following statement is correct. Already existing methods [41, 42, 43] are more than enough for its proof, which does not require any new ideas besides those presented in this chapter.

**Conjecture 4.4.3.** *Let the distribution of $X \in \Lambda$ be the Liouville measure $\mu(d\varphi ds) = Z^{-1}\cos(\varphi)d\varphi ds$. If*

$$\xi = \lim_{n\to\infty} \frac{x(T^n X) - x(X)}{g(n)}, \tag{4.20}$$

*then $\xi = (\xi_1, \xi_2)$ is a Gaussian random variable with zero mean where,*

1. *$g(n) = \sqrt{n}$ in case of finite horizon.*
2. *$g(n) = \sqrt{n \ln n}$ in case of infinite horizon but without corridors of type II.*
3. *$g(n) = \sqrt{n}\ln n$ in case of infinite horizon with presence of type II corridors.*

*Moreover, in item 3, when we consider the physical periodic Wind-Tree model presented in Section 4.3, the covariance matrix is given by*

$$\begin{bmatrix} D_{11} & D_{12} \\ D_{21} & D_{22} \end{bmatrix} = \begin{bmatrix} \frac{2ad_o^2}{|\partial S'|} & 0 \\ 0 & \frac{2ad_o^2}{|\partial S'|} \end{bmatrix}.$$

An outline of the proof in case of infinite horizon with presence of corridors of type II is as follows. According to Proposition 4.1.3, the probability distribution $\nu$ is symmetric, i.e. $\langle\xi\rangle = 0$. To find the covariance matrix, we need to calculate its components in corridors. There are four corridors in the physical periodic Ehrenfests' Wind-Tree model: $C_h$, $C_v$, $C_o^+$, and $C_o^-$. It follows from Section 4.2 that asymptotics of the probability distribution in $C_h$ and $C_v$ are the same as those in corridors of the Lorentz gas. Thus, with normalization $\sqrt{n}\ln(n)$ used in (4.20) and the result from [41], we will have $\langle\xi_i\xi_j\rangle = 0$ for $i, j = 1, 2$ when $\xi$ is in $C_h$ or $C_v$. This means, $D_{ij} = \langle\xi_i\xi_j\rangle$ only depends on the value $\langle\xi_i\xi_j\rangle_o$ where

$\xi$ is in $C_o^+$ or $C_o^-$. Let $\xi$ be in $C_o^+$, then:

$$\xi_1 \simeq \xi_2, \tag{4.21}$$

and,

$$\langle \xi_1 \xi_2 \rangle_o = \langle \xi_1^2 \rangle_o. \tag{4.22}$$

Similarly, when $\xi$ is in $C_o^-$:

$$\xi_1 \simeq -\xi_2, \tag{4.23}$$

and,

$$\langle \xi_1 \xi_2 \rangle_o = -\langle \xi_1^2 \rangle_o. \tag{4.24}$$

From (4.22) and (4.24), it follows that:

$$D_{12} = D_{21} = sum\ of\ values\ of\ \langle \xi_1 \xi_2 \rangle_o\ along\ C_o^+\ and\ C_o^- = 0$$

On the other hand, (4.21) and (4.23) imply that,

$$\xi_i^2 \simeq \frac{|\xi|^2}{2}, \tag{4.25}$$

for $i = 1, 2$.

By making use of (4.16), (4.19), and (4.25) and Proposition 4.3.2, one gets:

$$\begin{aligned} D_{11} = D_{22} =& sum\ of\ values\ of\ \langle \xi_1^2 \rangle_o\ along\ C_o^+\ and\ C_o^- = 2\langle \xi_1^2 \rangle_o = \langle |\xi|^2 \rangle_o \\ =& \langle \lim_{n\to\infty} \frac{|x(T^n X) - x(X)|^2}{n(\ln(n))^2} \rangle_o = \lim_{n\to\infty} \frac{\langle |x(T^n X) - x(X)|^2 \rangle_o}{n(\ln(n))^2} \\ =& \lim_{n\to\infty} \frac{n\langle |r(X)|^2 \rangle_o + 2\sum_{j=1}^{n-1}(n-j)\langle (r(X), r(T^j X)) \rangle_o}{n(\ln(n))^2} \\ =& \lim_{n\to\infty} \frac{2\sum_{j=1}^{n-1}\langle (r(X), r(T^j X)) \rangle_o}{(\ln(n))^2} = \frac{4ad_o^2}{Z} = \frac{2ad_o^2}{|\partial S'|}. \end{aligned}$$

### 4.4.3 Statistical Behavior of Trajectories in Continuous-Time Dynamics

In this section, we will present an analogous formula to (4.20) for continuous-time dynamics. Let $t_n$ be the time of the $n^{th}$ reflection of the trajectory $x(t)$. Then, $x(t_n) = x_n = x(X_n)$. Since the path of the particle between reflections is a line segment and the particle moves with velocity $1$ along it,

$$t_{n+1} - t_n = |x_{n+1} - x_n| = |r(X_n)|,$$

and,

$$t_n = \sum_{i=0}^{n-1} |r(T^i X_0)| = \sum_{i=0}^{n-1} |r(X_i)|.$$

For an arbitrary initial condition $X_0$, the ergodic theorem guarantees that,

$$\lim_{n\to\infty} \frac{t_n}{n} = \lim_{n\to\infty} \frac{\sum_{i=0}^{n-1} |r(X_i)|}{n} = \langle |r(X_0)| \rangle.$$

From Proposition 4.3.2, $\eta := \langle |r(X_0)| \rangle < \infty$. Therefore,

$$\lim_{n\to\infty} \frac{t_n (\ln t_n)^2}{n (\ln n)^2} = \eta,$$

and

$$\lim_{n\to\infty} \frac{t_{n+1} (\ln t_{n+1})^2}{t_n (\ln t_n)^2} = 1.$$

Let $t_n \le t < t_{n+1}$. It follows from lemma 7.1 in [41] and last two equations that,

$$\lim_{n\to\infty} \frac{x_t - x_0}{\sqrt{t} \ln t} = \lim_{n\to\infty} \frac{x_t - x_0}{\sqrt{t_n} \ln t_n} = \eta^{-1/2} \lim_{n\to\infty} \frac{x_t - x_0}{\sqrt{n} \ln n}. \tag{4.26}$$

The assumption $t_n \leq t < t_{n+1}$ implies that $x_t$ belongs to the segment $[x_n, x_{n+1}]$. Hence, $|x_t - x_n| \leq |r(X_n)|$. Thus almost surely,

$$\lim_{n\to\infty} \frac{x_t - x_n}{\sqrt{n}\ln n} = 0.$$

Therefore,

$$\lim_{n\to\infty} \frac{x_t - x_0}{\sqrt{n}\ln n} = \lim_{n\to\infty} \frac{x_n - x_0}{\sqrt{n}\ln n} = \xi.$$

where $\xi$ is the same as in Conjecture. Then, it follows from (4.26) that,

$$\lim_{t\to\infty} \frac{x_t - x_0}{\sqrt{t}\ln t} = \frac{\xi}{\sqrt{\eta}}.$$

This expression is analogous to (4.20) when we consider the continuous-time dynamics, and it shows that there is a new superdiffusive regime in the physical periodic Ehrenfests' Wind-Tree model where the diffusion coefficient $D(t) \sim (\ln t)^2$.

# CHAPTER 5
# BRIDGE TO HYPERBOLIC POLYGONAL BILLIARDS

In the last years, there has been significant research on billiards in polygons [52, 53, 54, 55, 56, 57, 58]. Dynamics of these models is extremely difficult to rigorously analyze which often happens with systems with intermediate, neither regular (integrable) nor chaotic, behavior.

In [10], it has been shown that the transition to physical billiards can completely change the dynamics. Moreover, any type of chaos-order or order-chaos transition may occur. In particular, it has been shown that classical Ehrenfests' Wind-Tree gas has richer dynamics than the Lorentz gas if a moving particle is real (physical) [11]. In this chapter, we show that typical physical billiard in polygons is chaotic for an arbitrarily small size (radius) of a moving particle. The last means that physical billiards in generic polygons are hyperbolic on a subset of positive measure and, particularly, have a positive Kolmogorov-Sinai entropy to the contrary to mathematical billiards in polygons, which have zero KS-entropy.

## 5.1 Billiards in Polygons

Let $\mathbf{P}$ be the space of all closed polygons in $\mathbf{R}^2$ and $\mathbf{P}_n \subset \mathbf{P}$ denote the space of all polygons with $n$ vertices. Let $\{v_0,\ v_1,\ \ldots,\ v_{n-1}\}$ be the set of vertices of a polygon in $\mathbf{P}_n$. If we fix one side of this polygon on the $x$-axis and one of the vertices of that side at the origin (e.g. $v_0 = (0,0)$ and $v_{n-1} = (x,0)$) then the embedding $\mathbf{P}_n \to \mathbf{R}^{2n-3}$ induces a topology in $\mathbf{P}_n$ such that its corresponding metric makes the space $\mathbf{P}_n$ complete [59]. If all angles of a polygon are commensurate with $\pi$, then it is called a rational polygon. It is well-known that rational polygons are dense in $\mathbf{P}$.

The phase space of this dynamical system is

$$\Lambda_P = \{(x, \varphi) \in \partial P \times (\frac{-\pi}{2}, \frac{\pi}{2}) \ : \ x \ is \ not \ a \ vertex \ of \ P\},$$

where $\varphi$ is the reflection angle with respect to the inward normal vector $n(x)$ to the boundary at reflection point $x \in \partial P$.

Let $\gamma$ be a billiard orbit in the polygon $P$. If the orbit $\gamma$ hits a side of the boundary $\partial P$ then instead of reflecting the orbit $\gamma$ off that side of $P$, one may reflect $P$ about that side. Denote the reflected polygon by $P_1$. The unfolded orbit $\gamma$ is a straight line as the continuation of $\gamma$ in $P_1$. In the geometric optics this procedure is called the method of images or unfolding [60]. Continuing this procedure for $n$ consecutive reflections of the orbit $\gamma$, we obtain a sequence of polygons $P,\ P_1,\ P_2, \ldots,\ P_n$ where the unfolded orbit $\gamma$ is a straight segment through $P_1$ to $P_n$ (Fig. 5.1).

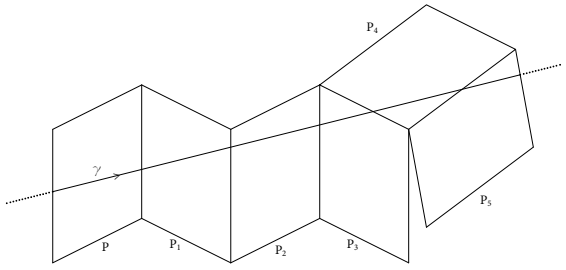


Figure 5.1: The unfolding process.

The unfolding process can also be done backward in time. A trajectory stops when it hits a vertex. The unfolded orbit $\gamma$ is a finite segment if it hits vertices of $P$ both in the future and in the past. Such trajectories are called *generalized diagonals*. In [59, 60], it is shown that the set of generalized diagonals of the polygon $P \in \mathbf{P}$ is countable.

Consider $(x, \varphi) \in \Lambda_P$. A direction $\varphi$ at point $x$ is called an *exceptional direction* if its trajectory hits a vertex of $P$. It is not difficult to see that the number of these exceptional directions is countable at each point $x$.

## 5.2 Physical Billiards in non-Convex Polygons

It is easy to see that dynamics of a physical billiard in a convex simply connected polygon is completely equivalent to dynamics of a mathematical billiard in this polygon [10]. However, the situation is totally different for non-convex polygons (more precisely, polygons with at least one reflex angle, see Fig. 5.2). In this case, the boundary of the equivalent mathematical billiard acquires some dispersing parts, which are arcs of a circle of radius $r$ (see e.g. [51, 61]).

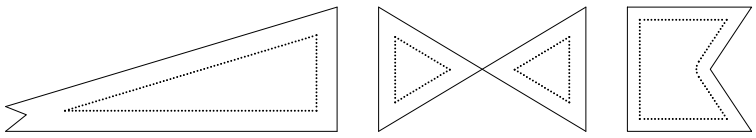

Figure 5.2: To have dispersing parts in the boundary of mathematical billiards equivalent to physical billiards in non-convex polygons, the particle has to be small enough and the polygon has to have at least one reflex angle.

Let $\mathbf{P}_{ref}$ be the set of all polygons that they have at least one reflex angle. To show that $\mathbf{P}_{ref}$ is dense in $\mathbf{P}$, we use the metric $d(.,.)$ on $\mathbf{P}$ which is defined as:

$$d(P,Q) = \int_{\mathbf{R}^2} |\chi_P(x) - \chi_Q(x)| dx, \tag{5.1}$$

where $P, Q \in \mathbf{P}$ and,

$$\chi_P(x) = \begin{cases} 1 & x \in P, \\ 0 & otherwise. \end{cases}$$

The topology induced by the metric $d(.,.)$ in $\mathbf{P}_n$ is equivalent to the induced topology in $\mathbf{P}_n$ by the embedding $\mathbf{P}_n \to \mathbf{R}^{2n-3}$. Thus, rational polygons are dense in $\mathbf{P}$ with respect to the metric $d(.,.)$.

**Lemma 5.2.1.** $\mathbf{P}_{ref}$ *is dense in* $\mathbf{P}$.

*Proof.* Let $P \in \mathbf{P}$ be a polygon with $n$ vertices $\{v_0,\ v_1,\ \ldots,\ v_{n-1}\}$. Without loss of generality, we assume that the randomly chosen edge of $P$ is $v_0v_{n-1}$. On the perpendicular

bisector of $v_0v_{n-1}$ in the interior of $P$, we choose a sequence of points $\{v_{n_k}\}_{k=k_0}^{\infty}$ such that the reflex angle $\angle v_0v_{n_k}v_{n-1} = \pi + \frac{\pi}{k}$ ($k_0$ is big enough to have $v_{n_k}$ for $k \geq k_0$ in the interior of $P$, see Fig. 5.3).

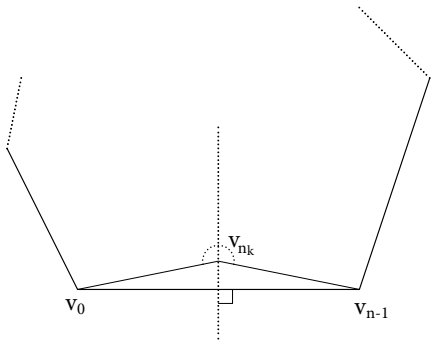


Figure 5.3: Replacing one edge of a polygon by a reflex angle.

If we denote the non-convex polygons with vertices $\{v_0,\ v_1,\ \ldots,\ v_{n-1},\ v_{n_k}\}$ by $P_k$ then it follows that $P_k \in \mathbf{P}_{ref}$ and

$$d(P, P_k) \to 0,$$

as $k \to \infty$. □

**Lemma 5.2.2.** $\mathbf{P}_{ref}$ *is open in* $\mathbf{P}$.

*Proof.* It is easy to see that any perturbation of $P \in \mathbf{P}_{ref}$ will have at least one reflex angle. This means $\mathbf{P}_{ref}$ is open in $\mathbf{P}$. □

Continued fractions for billiards were introduced in Sinai's fundamental paper [3]. They serve as a basic tool for analysis of billiards dynamics. Let $0 = t_0 < t_1 < t_2 < \ldots$ be the reflection times of the trajectory $\gamma$ off the boundary $\partial Q$ where $Q$ is an arbitrary billiard table. Denote by $\kappa_i$ the curvature of the boundary at the $i$th reflection point with respect to the inward unit normal vectors $n(x)$ to the boundary at $x \in \partial Q$, and by $\varphi_i$ the $i$th reflection angle such that $\frac{-\pi}{2} < \varphi_i < \frac{\pi}{2}$. The corresponding continued fraction of this trajectory is

given by

$$\varkappa = \cfrac{1}{\tau_1 + \cfrac{1}{\cfrac{2\kappa_1}{\cos\varphi_1} + \cfrac{1}{\tau_2 + \cfrac{1}{\cfrac{2\kappa_2}{\cos\varphi_2} + \cfrac{1}{\tau_3 + \cfrac{1}{\ddots}}}}}},$$

where $\tau_i = t_i - t_{i-1}$ for $i = 1, 2, \ldots$.

Let $P \in \mathbf{P}_{ref}$, then the curvature of boundary components of the mathematical billiard equivalent to the physical billiard in $P$ is either $0$ or $\frac{1}{r}$. If an orbit hits the dispersing components infinitely many times where reflection numbers on dispersing parts are given by the sequence $\{i_k\}_{k=1}^{\infty}$, then the continued fraction of this orbit will have the following form between $i_j$th and $i_{j+1}$th reflections,

$$\ddots + \cfrac{1}{\cfrac{2}{r\cos\varphi_{i_j}} + \cfrac{1}{(\tau_{i_j+1} + \cdots + \tau_{i_{j+1}}) + \cfrac{1}{\cfrac{2}{r\cos\varphi_{i_{j+1}}} + \cfrac{1}{\ddots}}}}.$$

All elements of continued fractions in this case are positive. Also, almost any orbit has finitely many reflections within any finite time interval, since the boundary components are $C^{\infty}$ (they are line segments or arcs of a circle of radius $r$). Therefore,

$$\sum_{k=0}^{\infty} \left( (\tau_{i_k+1} + \cdots + \tau_{i_{k+1}}) + \frac{2}{r\cos\varphi_{i_{k+1}}} \right) = \infty, \tag{5.2}$$

where $i_0 = 0$.

Let $\hat{\mathbf{P}}$ denote the space of all non-convex simply connected rational polygons. Then, $\hat{\mathbf{P}} \subset \mathbf{P}_{ref}$.

**Theorem 5.2.3.** *For any $P \in \hat{\mathbf{P}}$, there exists $r_P > 0$ such that the physical billiard in $P$ is hyperbolic for all $r < r_P$.*

*Proof.* Let $P \in \hat{\mathbf{P}}$ have $n$ vertices. Assume $\{v_0,\ v_1, \ldots,\ v_{n-1}\}$ and $\{e_1 = v_0v_1,\ e_2 = v_1v_2, \ldots,\ e_n = v_{n-1}v_0\}$ are sets of its vertices and edges, respectively. Let

$$r_k = \min\{|v_k - x| \ :\ x \in e_i \ for\ i \neq k \ and\ i \neq k+1\},$$

where $|.|$ is the euclidean distance in $\mathbf{R}^2$ and $k = 0, 1, \ldots, n-1$ (if $k = 0$ then $i = 2, 3, \ldots, n-1$). It is easy to see that $r_k$ is well-defined since it is the minimum value of a continuous function on a compact set. Moreover, $r_k > 0$. If we let

$$r_P = \min\{\frac{r_0}{2}, \frac{r_1}{2}, \ldots, \frac{r_{n-1}}{2}\}, \tag{5.3}$$

then the hard ball of radius $r < r_P$ will be able to hit all edges of $P$. Therefore, when $r < r_P$ the boundary of the equivalent mathematical billiard has some dispersing components.

In fact, if a radius of the particle is sufficiently large then some parts of the boundary of a billiard table become "non-visible" to the particle. Therefore it does not matter for dynamics what is the exact structure of this "non-visible" boundary. Such situation may occur e.g. for polygons [62].

As long as a trajectory does not hit dispersing parts, it can be considered as a trajectory in the rational polygon $P'$ that shapes by replacing the dispersing components of the boundary by flat segments (Fig. 5.4). More precisely, angles $\theta$ and $\alpha$ satisfy the equation $\alpha = \frac{\pi+\theta}{2}$ and $\theta$ is commensurate with $\pi$, therefore, $\alpha$ is commensurate with $\pi$.

It is well-known that almost all orbits of billiards in rational polygons are spatially dense inside the billiard table [59, 63, 64]. Thus, all non-exceptional trajectories in $P'$ will hit all

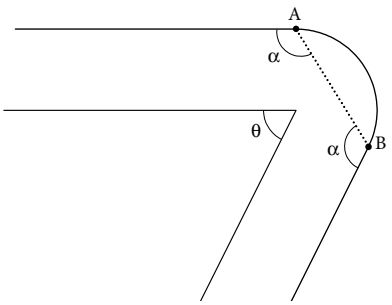


Figure 5.4: Replacing a dispersing part with a line segment.

edges of $P'$, including those replaced the dispersing parts of the boundary. This implies that almost all trajectories (full measure in phase space) in the mathematical billiard equivalent to the physical billiard in $P$ will hit at least one dispersing component. Note that after the first reflection off a dispersing component, the forward trajectory is not the same as the one in $P'$. Thus, we cannot use density of almost all orbits in $P'$ to show that the trajectory will hit dispersing parts of the boundary infinitely many times.

So, there is a full measure subset of points in the phase space such that their trajectories hit at least one dispersing component. Let $(x, \theta)$ be a point in that subset. By the continuity of the system on initial conditions, there is a neighborhood of positive measure of the point $(x, \theta)$ such that trajectories of all points in that neighborhood hit the same dispersing part as the trajectory of $(x, \theta)$ hits for the first time. Then the Poincare recurrence theorem implies that almost all trajectories in this neighborhood will return and hit that dispersing part infinitely many times. The convergence of continued fractions of such trajectories that hit dispersing components follows from the Seidel-Stern theorem and (5.2). Hence, for a full measure subset of the phase space of the physical billiard in non-convex simply connected rational polygons, we have hyperbolicity. Moreover, it implies there are at most countable number of ergodic components such that the Kolmogorov-Sinai entropy is positive on each of them [3, 65, 66]. □

It follows from Lemma 5.2.1 and 5.2.2 that $\mathbf{P}_{ref}$ is an open dense set in $\mathbf{P}$. Therefore, being a polygon with at least one reflex angle in $\mathbf{P}$ is topologically generic.

**Theorem 5.2.4.** *There is an open dense subset of* $\mathbf{P}$ *such that the physical billiard in the polygons of this subset (when the radius of the hard ball is small enough) is hyperbolic on a subset of positive measure of their phase spaces.*

*Proof.* Let $P \in \mathbf{P}_{ref}$ and $r_P > 0$ be the maximum radius of the hard ball defined in (5.3) such that the particle can hit all edges of $P$. Then the boundary of the mathematical billiard equivalent to the physical billiard in $P$ has some dispersing components which are arcs of a circle of radius $r < r_P$. Let,

$$A = \{(x, \varphi) \ : \ For\ all\ x\ in\ a\ dispersing\ component\ and\ \varphi \in (\frac{-\pi}{2}, \frac{\pi}{2})\}.$$

It follows from the definition of $A$ that it is a subset of positive measure in the phase space (one can exclude the exceptional directions which form a measure zero set in the phase space). The Poincare recurrence theorem implies that almost all points of $A$ will return to $A$ infinitely many times under the action of the billiard map. That means almost all trajectories of points in $A$ will hit a dispersing part infinitely many times. Then the convergence of continued fractions of trajectories of almost all points of $A$ follows from the Seidel-Stern theorem and (5.2). Hence a physical billiard in a polygon with a reflex angle is hyperbolic at least on a subset of positive measure of its phase space. □

We conjecture that in fact generically a physical billiard in polygon is ergodic for any radius of a moving particle (which is of course not that large that the particle cannot move within a polygon). To prove our conjecture one instead needs to show that almost all orbits in a physical billiard in a polygon will eventually hit any segment which is a part of any side of a polygon. Hence a "large" physical particle must hit all (rather than one) vertices of a polygon. For instance, if each vertex of a convex polygon gets replaced by a focusing arc it is possible to prove ergodicity [67]. In this case the mechanism of defocusing [68] ensures hyperbolicity of such semi-focusing billiards on entire phase space. The current theory of billiards in polygons establishes only that any billiard orbit in a polygon is either

periodic or its closer contains just one vertex of this polygon, which is by far not enough. We are confident though that our conjecture holds.

## REFERENCES


[1] G. Birkhoff, "Dynamical systems with two degrees of freedom," *Trans. Amer. Math.*, vol. 18, no. 2, pp. 199–300, 1917.

[2] ——, "On the periodic motions of dynamical systems," *Acta Math.*, vol. 50, no. 1, pp. 359–379, 1927.

[3] Y. Sinai, "Dynamical systems with elastic reflections," *Russian Mathematical Surveys*, vol. 25, pp. 137–189, 1970.

[4] C. Dettmann, E. Cohen, and H. V. Beijeren, "Statistical mechanics: Microscopic chaos from brownian motion?" *Nature*, vol. 401, pp. 875–875, 1999.

[5] E. Hauge and E. Cohen, "Normal and abnormal diffusion in ehrenfests' wind-tree model," *Journal of Mathematical Physics*, vol. 10, pp. 397–414, 1969.

[6] W. Wood and F. Lado, "Monte carlo calculation of normal and abnormal diffusion in ehrenfest's wind-tree model," *Journal of Computational Physics*, vol. 7, no. 3, pp. 528–546, 1971.

[7] G. Gallavotti and D. Ornstein, "Billiards and bernoulli schemes," *Comm. Math. Phys.*, vol. 38, pp. 83–101, 1974.

[8] H. Lorentz, "The motion of electrons in metallic bodies," *Proc. Amst. Acad.*, vol. 7, pp. 438–453, 585–593, 684–691, 1905.

[9] L. Boltzmann, "Weitere studien uber das warme gleichgenicht unfer gasmolakular," *Sitzungsberichte der Akademie der Wissenschaften*, vol. 66, pp. 275–370, 1872.

[10] L. Bunimovich, "Physical versus mathematical billiards: From regular dynamics to chaos and back," *Chaos*, vol. 29, p. 091 105, 2019.

[11] H. Attarchi, M. Bolding, and L. Bunimovich, "Ehrenfests' wind–tree model is dynamically richer than the lorentz gas," *J. Stat. Phys.*, vol. 180, pp. 440–458, 2020.

[12] S. Pilatowsky-Cameo, J. Chavez-Carlos, M. Bastarrachea-Magnani, P. Stransky, S. Lerma-Hernandez, L. Santos, and J. Hirsch, "Positive quantum lyapunov exponents in experimental systems with a regular classical limit," *Phys. Rev. E*, vol. 101, p. 010 202, 2020.

[13] E. Rozenbaum, L. Bunimovich, and V. Galitski, "Early-time exponential instabilities in nonchaotic quantum systems," *Phys. Rev. Lett.*, vol. 125, p. 014 101, 2020.

[14] G. Pianigiani and J. Yorke, "Expanding maps on sets which are almost invariant: Decay and chaos," *Trans. Am. Math. Soc.*, vol. 252, pp. 351–366, 1979.

[15] M. Demers and L.-S. Young, "Escape rates and conditionally invariant measures," *Nonlinearity*, vol. 19, pp. 377–397, 2006.

[16] E. Altmann, J. Portela, and T. Tél, "Leaking chaotic systems," *Rev. Mod. Phys.*, vol. 85, pp. 869–918, 2013.

[17] H. Attarchi and L. Bunimovich, "Why escape is faster than expected," *Journal of Physics A: Mathematical and Theoretical*, vol. 53, p. 435 002, 2020.

[18] ——, "Collision of a hard ball with singular points of the boundary," *Chaos*, vol. 31, p. 013 123, 2021.

[19] ——, "Bridge to hyperbolic polygonal billiards," *Pure and Applied Functional Analysis*, vol. 5, pp. 1249–1256, 2020.

[20] L. Bunimovich and A. Yurchenko, "Where to place a hole to achieve a maximal escape rate," *Israel Journal of Mathematics*, vol. 182, pp. 229–252, 2011.

[21] L. Bunimovich and L. Vela-Arevalo, "Some new surprises in chaos," *Chaos*, vol. 25, p. 097 614, 2015.

[22] O. Georgiou, C. Dettmann, and E. Altmann, "Faster than expected escape for a class of fully chaotic maps," *Chaos*, vol. 22, p. 043 115, 2012.

[23] A. Ferguson and M. Pollicott, "Escape rates for gibbs measures," *Ergod. Theory Dyn. Syst.*, vol. 32, pp. 961–988, 2012.

[24] G. Keller and C. Liverani, "Rare events, escape rates and quasistationarity: Some exact formulae," *J. Stat. Phys.*, vol. 135, pp. 519–534, 2009.

[25] R. Adler and B. Weiss, *Similarity of automorphisms of the torus*. Memoirs of the American Mathematical Society, 1970.

[26] S. Ulam, *Problems in Modern Mathematics*. Interscience, New York, 1964.

[27] Y. Sinai, "Gibbs measures in ergodic theory," *Russ. Math. Surv.*, vol. 27, pp. 21–69, 1972.

[28] V. Paar and N. Pavin, "Bursts in average lifetime of transients for chaotic logistic map with a hole," *Phys. Rev. E*, vol. 55, pp. 4112–4115, 1997.

[29] V. Afraimovich and L. Bunimovich, "Dynamical networks: Interplay of topology, interactions and local dynamics," *Nonlinearity*, vol. 20, pp. 1761–1777, 2007.

[30] Y. Bakhtin and L. Bunimovich, "The optimal sink and the best source in a markov chain," *J. Stat. Phys.*, vol. 143, pp. 943–954, 2011.

[31] V. Afraimovich and L. Bunimovich, "Which hole is leaking the most: A topological approach to study open systems," *Nonlinearity*, vol. 23, pp. 643–656, 2010.

[32] R. Garwin, "Kinematics of an ultraelastic rough ball," *Am. J. Phys.*, vol. 37, pp. 88–92, 1969.

[33] D. Broomhead and E. Gutkin, "The dynamics of billiards with no-slip collisions," *Physica D*, vol. 67, pp. 188–197, 1993.

[34] C. Cox and R. Feres, *No-slip billiards in dimension two*. Amer. Math. Soc., 2017.

[35] P. Ehrenfest and T. Ehrenfest, "Begriffliche grundlagen der statistischen auffassung in der mechanik," *Encykl. d. Math. Wissensch*, vol. 6, p. 90, 1912.

[36] C. Bianca and L. Rondoni, "The nonequilibrium ehrenfest gas: A chaotic model with flat obstacles?" *Chaos*, vol. 19, p. 013 121, 2009.

[37] G. Gallavotti, "Divergences and the approach to equilibrium in the lorentz and the wind-tree models," *Phys. Rev.*, vol. 185, pp. 308–322, 1969.

[38] H. V. Beyeren and E. Hauge, "Abnormal diffusion in ehrenfest's wind-tree model," *Physics Letters A*, vol. 39, no. 5, pp. 397–398, 1972.

[39] V. Delecroix, "Divergent trajectories in the periodic wind-tree model," *J. Mod. Dyn.*, vol. 7, pp. 1–29, 2013.

[40] V. Delecroix, P. Hubert, and S. Lelievre, "Diffusion for the periodic wind-tree model," *Ann. Sci.*, vol. 47, pp. 1085–1110, 2014.

[41] P. Bleher, "Statistical properties of two-dimensional periodic lorentz gas with infinite horizon," *Journal of Statistical Physics*, vol. 66, pp. 315–373, 1992.

[42] L. Bunimovich and Y. Sinai, "Statistical properties of lorentz gas with periodic configuration of scatterers," *Commun. Math. Phys.*, vol. 78, pp. 479–497, 1981.

[43] L. Bunimovich, Y. Sinai, and N. Chernov, "Statistical properties of two-dimensional hyperbolic billiards," *Russian Math. Surveys*, vol. 46, no. 4, pp. 47–106, 1991.

[44] A. Avila and P. Hubert, "Recurrence for the wind-tree model," *Annales de l'Institut Henri Poincare C- Analyse non lineaire*, vol. 37, no. 1, pp. 1–11, 2020.

[45] K. Fraczek and C. Ulcigrai, "Non-ergodic z-periodic billiards and infinite translation surfaces," *Invent. Math.*, vol. 197, pp. 241–298, 2014.

[46] J. Hardy and J. Weber, "Diffusion in a periodic wind-tree model," *Journal of Mathematical Physics*, vol. 21, pp. 1802–1808, 1980.

[47] P. Hooper, P. Hubert, and B. Weiss, "Dynamics on the infinite staircase discrete," *Contin. Dyn. Syst.*, vol. 33, pp. 4341–4347, 2013.

[48] P. Hubert, S. Lelie'vre, and S. Troubetzkoy, "The ehrenfest wind-tree model: Periodic directions, recurrence, diffusion," *J. Reine Angew. Math.*, vol. 656, pp. 223–244, 2011.

[49] P. Hubert and B. Weiss, "Ergodicity for infinite periodic translation surfaces," *Compos. Math.*, vol. 149, pp. 1364–1380, 2013.

[50] D. Ralston and S. Troubetzkoy, "Ergodic infinite group extensions of geodesic flows on translation surfaces," *J. Mod. Dyn.*, vol. 6, pp. 477–497, 2012.

[51] C. Cox, R. Feres, and H. Zhang, "Stability of periodic orbits in no-slip billiards," *Nonlinearity*, vol. 31, pp. 4443–4471, 2018.

[52] J. Bobok and S. Troubetzkoy, "Code & order in polygonal billiards," *Topology Appl.*, vol. 159, pp. 236–247, 2012.

[53] M. Boshernitzan, G. Galperin, T. Kruger, and S. Troubetzkoy, "Periodic billiard orbits are dense in rational polygons," *Transactions AMS*, vol. 350, pp. 3523–3535, 1998.

[54] K. Fraczek and C. Ulcigrai, "Ergodic directions for billiards in a strip with periodically located obstacles," *Comm. Math. Phys.*, vol. 327, pp. 643–663, 2014.

[55] K. Fraczek, R. Shi, and C. Ulcigrai, "Genericity on curves and applications: Pseudo-integrable billiards, eaton lenses and gap distributions," *J. Mod. Dyn.*, vol. 12, pp. 55–122, 2018.

[56] G. Galperin, "Nonperiodic and not everywhere dense billiard trajectories in convex polygons and polyhedrons," *Comm. Math. Phys.*, vol. 91, pp. 187–211, 1983.

[57] A. Skripchenko and S. Troubetzkoy, "Polygonal billiards with one sided scattering," *Ann. Inst. Fourier*, vol. 65, pp. 1881–1896, 2015.

[58] Y. Vorobets, "Ergodicity of billiards in polygons," *Sb. Math.*, vol. 188, no. 3, pp. 389–434, 1997.

[59] A. Zemlyakov and A. Katok, "Topological transitivity of billiards in polygons," *Math. Notes*, vol. 18, pp. 760–764, 1975.

[60] E. Gutkin, "Billiards in polygons," *Phys. D*, vol. 19, pp. 311–333, 1986.

[61] C. Cox and R. Feres, "Differential geometry of rigid bodies collisions and non-standard billiards," *Discrete & Continuous Dynamical Systems-A*, vol. 36, pp. 6065–6099, 2016.

[62] P. Balint and S. Troubetzkoy, "Ergodicity of two hard balls in integrable polygons," *Nonlinearity*, vol. 17, pp. 2069–2090, 2004.

[63] C. Boldrighini, M. Keane, and F. Marchetti, "Billiards in polygons," *Ann. Probab.*, vol. 6, pp. 532–540, 1978.

[64] S. Kerckhoff, H. Masur, and J. Smillie, "Ergodicity of billiard flows and quadratic differentials," *Ann. of Math.*, vol. 124, pp. 293–311, 1986.

[65] L. Bunimovich and Y. Sinai, "On the main theorem of the ergodic theory of dispersing billiards," *Math. USSR Sbornik*, vol. 19, pp. 407–423, 1973.

[66] L. Bunimovich, "A theorem on ergodicity of two-dimensional hyperbolic billiards," *Comm. Math. Phys.*, vol. 130, pp. 599–621, 1990.

[67] N. Chernovy and S. Troubetzkoy, "Ergodicity of billiards in polygons with pockets," *Nonlinearity*, vol. 11, pp. 1095–1102, 1998.

[68] L. Bunimovich, "On billiards close to dispersing," *Mat. USSR Sbornik*, vol. 23, pp. 45–67, 1974.

# VITA

Hassan Attarchi was born in Gorgan, Iran, in 1984. He attended Amirkabir University of Technology (Tehran Polytechnic), where he received a Ph.D. degree in Mathematics in 2012. In 2016 he entered the second Ph.D. program in Mathematics at Georgia Tech. Here he worked on dynamical systems of the billiard type under the direction of Prof. Leonid A. Bunimovich. He plans to graduate in the Summer 2021. He accepted a visiting assistant professor position at University of California, Riverside.